JOURNAL OF GEOPHYSICAL RESEARCH, VOL. 111, F03002, doi:10.1029/2005JF000294, 2006

Use of a regional, relict landscape to measure vertical deformation of the eastern Tibetan Plateau

M. K. Clark,[1,2] L. H. Royden,[1] K. X. Whipple,[1] B. C. Burchfiel,[1] X. Zhang,[3] and W. Tang[3]

Received 7 February 2005; revised 27 December 2005; accepted 16 February 2006; published 8 July 2006.

[1] Field work and topography analysis show that remnant, local areas of a low-relief landscape or erosion surfaces are geographically continuous across the southeastern Tibetan Plateau margin. We correlate these remnant surfaces as a paleolandscape that formed at low elevation. Remnants of this paleolandscape are preserved because incision of the fluvial system has been largely limited to major rivers and principal tributaries and has not yet progressed throughout the entire fluvial network. The incomplete adjustment of the fluvial system signals initiation of rapid bedrock incision into a developing plateau margin, and erosional denudation is concentrated in the major river channels. This interpretation contradicts earlier notions that low-gradient, regional topography is the product of regional elevation reduction by intense landscape dissection due to the presence of several large southeast flowing rivers. The modern altitude of the reconstructed paleolandscape (or ''relict landscape'') constrains the vertical displacement of the plateau surface in response to crustal thickening and subsequent erosion during the lateral growth of the Tibetan Plateau. Regional preservation of the relict landscape is consistent with minor surface disruption by late Cenozoic thrust faults and folds and supports a model of distributed lower crustal thickening. Because significant erosion is limited to narrow river gorges, an increase in the plateau elevation due to isostatic rebound is minor. Therefore we propose that the modern elevation of the relict landscape reflects isostatically compensated thickening of the lower crust.

Citation: Clark, M. K., L. H. Royden, K. X. Whipple, B. C. Burchfiel, X. Zhang, and W. Tang (2006), Use of a regional, relict landscape to measure vertical deformation of the eastern Tibetan Plateau, *J. Geophys. Res.*, *111*, F03002, doi:10.1029/2005JF000294.

1. Introduction

[2] The landscape of eastern Tibet is highly unusual; it stands at high elevation and is drained by four of the world's largest rivers, yet it has experienced little erosion in Cenozoic time (Figures 1 and 2) [*Von Lóczy*, 1893; *Gregory and Gregory*, 1925; *Barbour*, 1936; *Tregar*, 1965; *Wang et al.*, 1998]. Most of the erosion is limited to deep gorges formed by the major rivers and their principal tributaries. The unincised areas that surround the river gorges take the form of low-relief upland surfaces that are broadly distributed across the plateau margin. Collectively, these low-relief areas form a discontinuous, regional surface that defines the maximum elevation of the plateau margin from elevations of 5 km to sea level where it merges with the coastal plain (Figures 2 and 3). The continuity of such features argues against the notion that lower elevations in southeastern Tibet are due to a completely dissected, erosionally lowered topography or to models of stepwise, west-to-east growth of the southeastern plateau [*Fielding*, 1996; *Tapponnier et al.*, 2001].

[3] These low-relief upland surfaces are located in the upstream portions of major rivers and tributary basins, suggesting that their preservation is due to recent acceleration of river incision that has not yet progressed entirely through the drainage network. In this view, the juxtaposition of low-relief upland surfaces with deeply incised river gorges, is a product of a transitional landscape that is responding, but not yet fully adjusted, to a change in surface elevation (Figure 4). While this type of transitional landscape can be observed in many other localities, the extreme elevation and lateral extent of the Tibetan Plateau make eastern plateau margin the most dramatic example of such landscape [e.g., *Lawson*, 1936; *Webb*, 1946; *Epis and Chapin*, 1975; *Gansser*, 1983; *Gubbels et al.*, 1993; *Chapin and Kelley*, 1997; *Abbott et al.*, 1997; *Sugai and Ohmori*, 1999].

[4] In this paper, we outline how low-relief upland surfaces can be interpreted to represent the paleolandscape of the eastern Tibetan plateau prior to the rise of the plateau to its modern elevation. Reconstruction of this paleolandscape provides a reference datum that allows us to measure the spatial distribution of vertical displacement that has occurred in response to crustal thickening. This record of vertical displacement provides constraints on models of

[1]Department of Earth, Atmospheric and Planetary Sciences, Massachusetts Institute of Technology, Cambridge, Massachusetts, USA.
[2]Now at Department of Geological Sciences, University of Michigan, Ann Arbor, Michigan, USA.
[3]Chengdu Institute of Geology and Mineral Resources, Chengdu, China.

0148-0227/06/2005JF000294$09.00

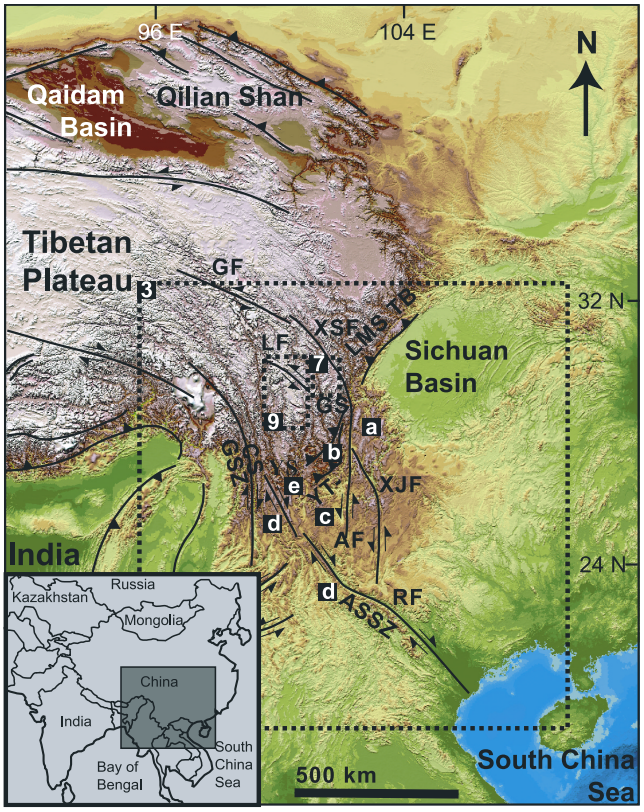

Figure 1. Topographic map of the eastern Tibetan Plateau and major geologic structures of Cenozoic age. Topography is derived from publicly available ~1 km resolution GTOPO30 digital elevation model [*U.S. Geological Survey*, 1993]. Inset boxes refer to later figures given by the number in each box (i.e., Figures 3, 7, and 9). Letters refer to basin locations and abbreviations refer to faults as follows: a, Daliang Basin; b, Yanyuan Basin; c, Chuxiong Basin; d, Lanping–Simao Basin; e, Jianchuan Basin; GF, Ganzi Fault; XSF, Xianshuihe Fault; LF, Litang Fault; XJF, Xiaojiang Fault; AF, Anning Fault; YT LMS TB, Ya-long–Longmen Shan Thrust Belt; RF, Red River Fault; ASSZ, Ailao Shan Shear Zone; GSZ, Gaoligong Shear Zone; CS, Chongshan Shear Zone; YS, Yulong-Snow Mountains; GS, Gonga Shan.

plateau growth and models that relate plateau growth to changes in regional climate. Thus the geomorphology of the eastern Tibetan Plateau provides an opportunity to demonstrate how reconstructed paleolandscapes can be used in regional tectonic studies. Although the focus of this paper is on the identification and correlation of landforms that define a paleolandscape, the reconstruction of the relict landscape in eastern Tibet has been used as a vertical datum to constrain models of crustal dynamics [*Clark and Royden*, 2000; *Clark et al.*, 2004, 2005a].

2. Use of Landscape Surfaces as a Reference Datum

[5] *Davis* [1899] defined the peneplain as the final product of landscape evolution, when a landscape grades by fluvial erosion to sea level. Thus static, planar features in the landscape were interpreted as peneplains and used as an absolute horizontal datum which recorded elevation change with respect to sea level. Later derivatives of the peneplain concept each provided a newly recognized mechanism of generating a landscape of low relief (i.e., peneplanes, pediplains, etchplains, etc.) focusing on the genetic origin of these landforms as a means by which a paleolandscape horizon could be identified (see *Widdowson* [1997] for a review of paleosurface research). These early studies were provocative because they suggested a way in which ancient landscapes could be used to measure vertical displacements of the Earth's surface.

[6] As the understanding of landscape evolution has progressed, the concept of peneplains has been largely abandoned in modern geomorphic research. Reasons include the following: (1) Landscapes do not necessarily evolve to a static state, but are dynamic systems responding to a spatially and temporally variable continuum of tectonic and climatic conditions (see *Merritts and Ellis* [1994] for a review). Therefore, even at extremely slow erosion rates (<0.01 mm/yr), landscapes are never truly static. (2) Low-relief landscapes can grade to a local base level at any elevation and need not have formed near sea level. (3) Regional-scale landscapes are commonly polygenetic, forming through the superposition of genetically unrelated surface processes that involve more than one erosional or depositional process. For example, the juxtaposition of low-relief erosional landscapes and adjacent depositional ones is a common occurrence.

[7] These considerations have largely limited the modern application of the peneplain to local-scale "erosion surfaces," using a single, time-correlative erosional horizon to measure local vertical offsets [e.g., *Spotila and Sieh*, 2000]. The requirement that erosion surfaces be temporally and genetically correlated has effectively precluded the use of ancient, polygentic landscapes as reference datums. This is unfortunate because it prohibits the use of paleolandscapes as a measure of vertical displacements at regional scales.

[8] In order to make use of low-relief paleolandscapes in this way, we define a "relict landscape" as a collection of landforms that may have different origins and different ages, but that collectively formed a low-relief landscape at some time in the past. In the following discussion we refer to "remnant surface" as a portion of a once regionally continuous, low-relief landscape that is initially of erosional or depositional origin and that is associated with a protracted period of erosion [*Widdowson*, 1997]. Such relict landscapes can be identified by the spatial correlation of individual remnant surfaces. The goal of this paper is to describe and correlate individual remnant surfaces across the eastern Tibetan Plateau, and to use the reconstructed paleolandscape as a measure of vertical deformation in response to crustal thickening.

3. "Active" Versus "Relict" Landscapes

[9] Fluvial systems are remarkably sensitive indicators of changes in tectonic and/or climatic boundary conditions that set landscape form. Rivers respond to changes in forcing by a spatial propagation of new incision rates, channel and hillslope gradients, and dominant erosional processes active in the channel bed and on neighboring hillslopes. Before

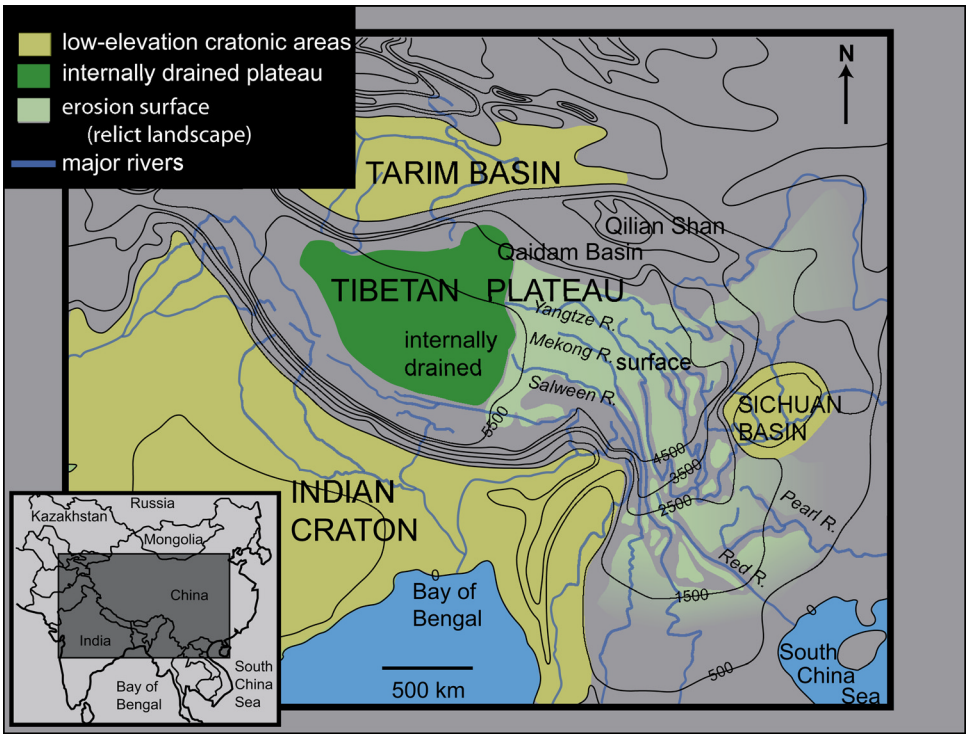

Figure 2. Geomorphic map of the Tibetan Plateau with smoothed elevation contours. Dark green region outlines internally drained west central plateau. Light green region shows extent of externally drained, low-relief relict landscape along eastern plateau. Yellow represents low-elevation cratonic areas that have experienced relatively minor Cenozoic deformation.

this adjustment is complete, there will exist a period of time in which part of the landscape has adjusted, or is adjusting to, new conditions and part has not. Thus in the most simple of terms, identification of paleolandscapes depends on our ability to make this distinction.

[10] The general contrast in the morphology of the eastern Tibetan Plateau landscape from low-relief, high-elevation "surfaces" to low-elevation, deeply dissected landscapes of the major river valleys is evident to even the casual observer (Figure 5). We define the "active" landscape as areas that are actively responding by increased fluvial erosion rates and mass wasting to the deep incision of the major rivers and principal tributaries. Erosion of the active landscape is driven by incision on the major rivers: the Salween, Mekong, Yangtze, Red and Pearl rivers (Figure 2). These rivers have carved impressive river canyons that are a maximum of 3–3.5 km deep (Figures 5e and 6b). We assume that this dramatic incision occurs in response to an increase in plateau elevation and favorable climate conditions.

[11] The active landscape contrasts sharply with low-relief areas that are spatially continuous across the plateau margin and are preserved at a range of elevations (Figures 3 and 6). These areas are generally low-relief, bedrock erosional surfaces with occasional Tertiary or Quaternary sedimentary cover. These surfaces make up the headwaters of many tributary rivers that transform downstream from alluvial to bedrock rivers where they become a part of the active landscape. Therefore surface remnants are not internally drained and isolated from the major fluvial systems, but are always located in the upstream portions of tributary basins and the headwaters of major rivers. This is a critical observation because it suggests that the spatial propagation of new erosional conditions has begun first on larger rivers with highest drainage areas, and has propagated into smaller tributaries with correspondingly lower drainage areas, and has not yet affected the low-relief surface remnants (Figures 5a–5d). Thus upland surfaces are interpreted as "relict" in the sense that they have not yet responded to modern base level fall set by the incision of the major rivers.

4. Mapping and Characterizing Relict Landscape (Surface) Remnants

[12] In this section, we describe a protocol for mapping surface remnants through an evaluation of elevation, slope and relief maps, CORONA imagery, 1:200,000 scale geologic maps, and field observations. We use a number of criteria to identify contrasting relict vs. active landscape elements, including: local elevation, local slope, local relief, active structures, and erosional processes. A summary of the general criteria used to identify remnant surfaces are found in Table 1. Some characteristics can be calculated and defined from computer algorithms using digital data, such as topographic relief and slope. Other characteristics were based on field observation which could not be carried out everywhere throughout the study area. However, we were able to associate field observations with characteristics in digital topography and imagery data that allowed us to extrapolate our analysis over large areas. Field observations

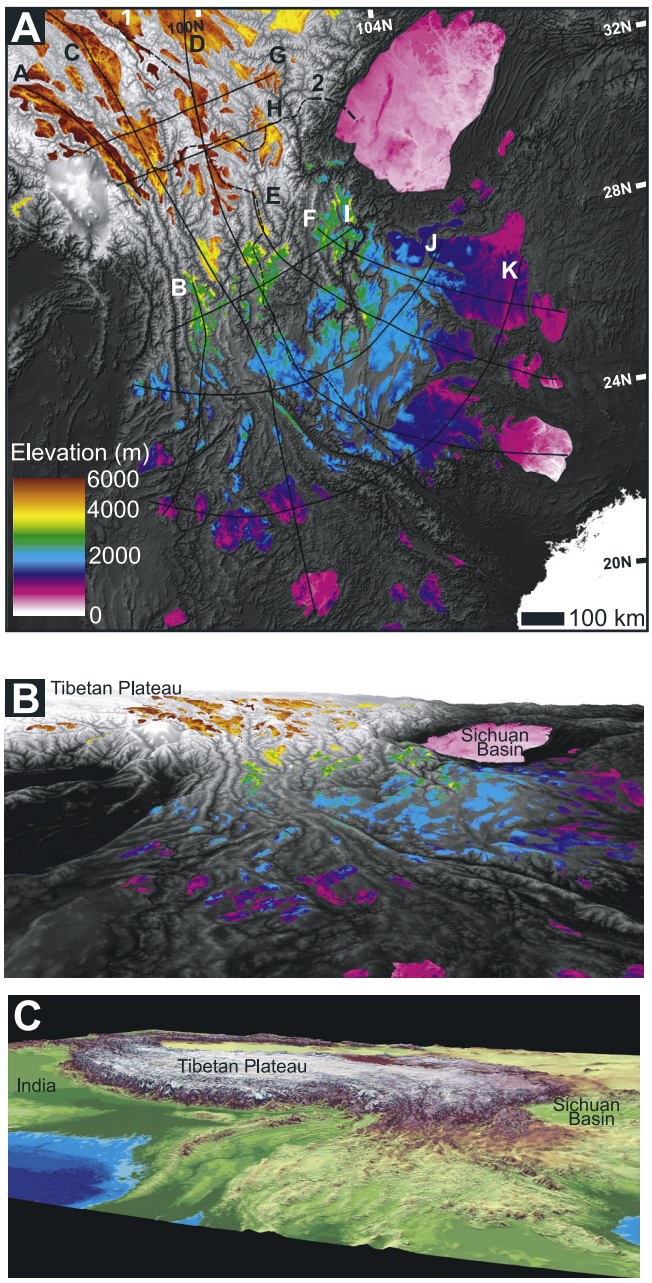

Figure 3. (a) Detailed elevation map of remnant surfaces draped over gray scale digital topography. Dashed lines (1–2) show location of cross sections in Figure 6. Solid lines (A–K) show locations of cross sections shown in Figures 11 and 12. (b) Three-dimensional perspective of topography. Close-up of southeastern plateau margin (gray scale topography) with surface remnants (color). Shown are the same map extent and map legend as in Figure 3a. (c) View of southeastern plateau highlighting the low regional topographic gradient of the southeastern plateau margin compared to the adjacent steep plateau margins to the west (Himalaya) and northeast (Longmen Shan).

and geologic data from maps were compared to the output of digital data and the resulting remnant surfaces were mapped by hand onto a topographic base map. The remainder of this section describes these criteria and how they were applied to map remnant surfaces. In the following section we summarize the geologic constraints and geomorphic descriptions by region that were used to constrain the age of relict surface formation and its subsequent abandonment following tectonic deformation.

[13] The active landscape is occupied by the major river valleys where bedrock terraces, bedrock or mixed rivers and massive landslides are common. Thin mantles of alluvium, mass-wasting debris, and boulder amour are also common on bedrock valley floors, as are occasional flights of alluvial terraces. Sediment storage in the river valleys is short-term and likely related to climatically or seismically induced mass-wasting events, which in some cases temporarily dam a river (i.e., the Xigada Formation [*Bureau of Geology and Mineral Resources of Sichuan Province* (*BGMRS*), 1991]). Sediment commonly accumulates locally in the river valley floor behind active strike-slip faults, but the total volume of this ponded sediment is small. In areas of erosionally less-resistant lithologies, such as late Mesozoic–early Tertiary sedimentary basins, wider, open valleys have developed with alluviated valley floors.

[14] The relict landscape is recognized by its more subdued local relief and erosional processes that are associated with slow erosion rates. CORONA images are high-resolution, black-and-white satellite photos with stereopairs and were used identify river channel morphology, such as channel and valley width, coarse estimates of bed load and dominant bed character (bedrock, mixed or alluvial), and vegetative cover. The data from these images and field observations suggest that hillslope creep, alluvial (transport

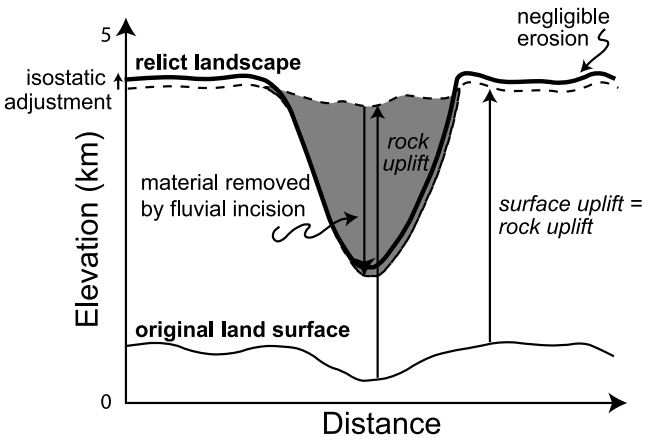

Figure 4. Cartoon cross section of landscape evolution of the east Tibetan Plateau. As mean elevation increases, the low-relief paleolandscape is elevated and becomes a relict landscape as rivers respond to new conditions by incising deep river canyons. Thin line represents low-relief paleolandscape that becomes elevated during crustal thickening (dashed line). A small amount of isostatic adjustment occurs because of the evacuation of the river gorges and rise of the surrounding, minimally eroded relict landscape, resulting in the modern landscape (thick line). Remnants of the relict landscape are preserved because the adjustment of fluvial channels to new conditions set by the modern high elevations is not complete. Where remnant surfaces of the relict landscape exist, their change in elevation represents both surface and rock uplift.

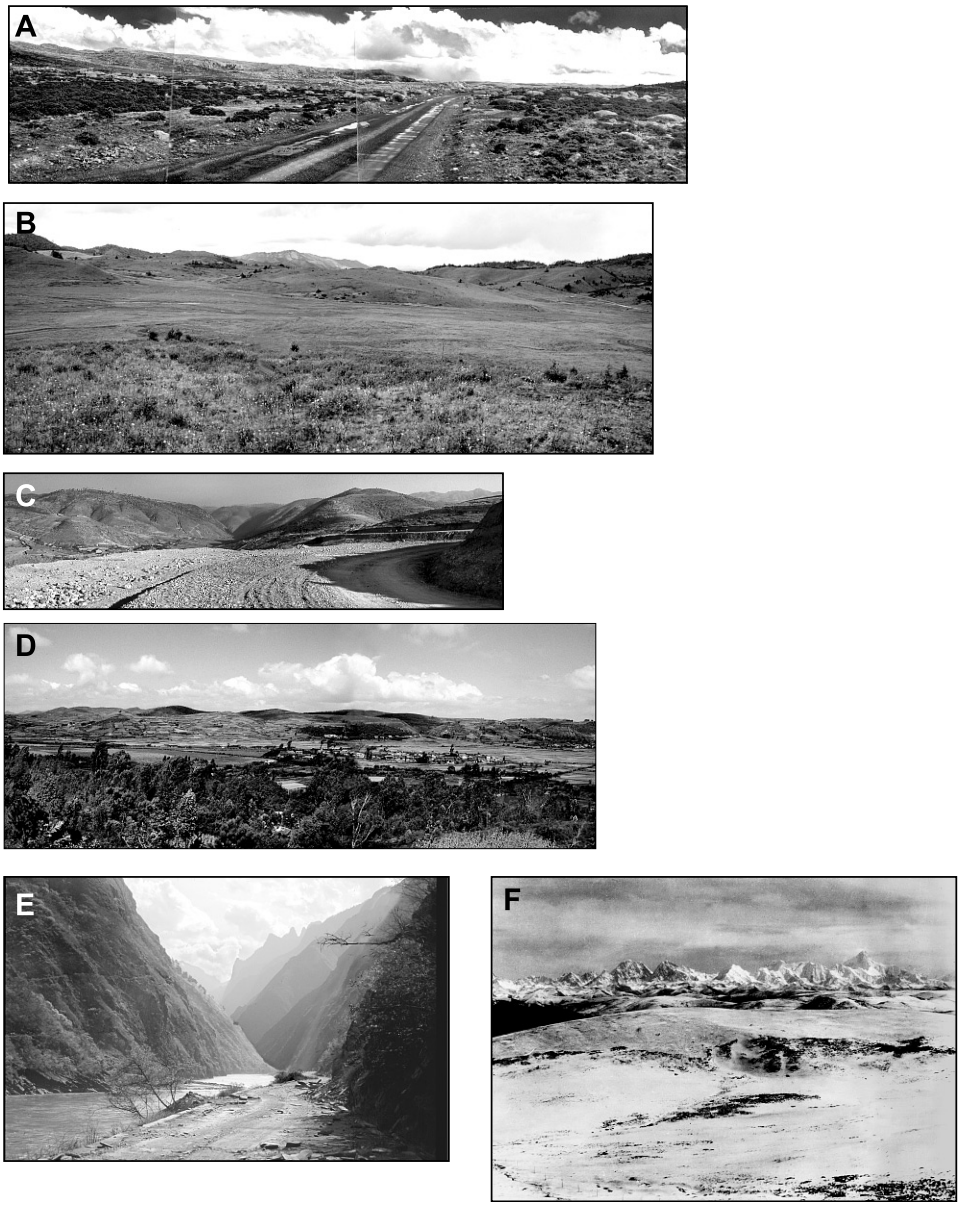

Figure 5. Field examples of remnant surfaces (relict landscape), deep river gorges (active landscape), and anomalously high topography at the steep plateau margin. (a) Remnant surface at 4700 m elevation, Songpan-Garze terrane. (b) Remnant surface at 4000 m elevation, between the Mekong and Yangtze rivers. (c) Remnant surface at 3000 m elevation, Yanyuan Basin. Low-relief landscape encompasses entire view. (d) Remnant surface at 2000 m elevation, the South China Fold and Thrust Belt. (e) Yalong River gorge, elevation 1600 m. (f) View east across remnant surface (4200 m elevation) at high-relief topography of the Gonga Shan massif (5500–7756 m) which interrupts the remnant surface (photograph by A. Heim (1932, ETH library, Zürich, call number Hs 494b:25 290)). Gonga Shan is located at the plateau margin near the southwestern corner of the Sichuan Basin and is a local area associated with young faulting, magmatism, and rapid late Miocene exhumation rates [*Niemi et al.*, 2003; *Roger et al.*, 1995].

limited) rivers, and chemical weathering that produces thick soils or saprolite dominate the erosional processes across remnant surfaces. Glacial erosion is observed only locally, particularly where the surface elevation is in excess of 5000–5500 m elevation. Much of the areal extent of the eastern plateau has no evidence of ice occupation [*Lehmkuhl*, 1998]. Furthermore, preservation of Tertiary sedimentary rocks and isotopic dating of rocks on the remnant surfaces at high elevation suggest that glacial sculpting has not caused significant net erosion. Altiplanation or cyroplanation, where smoothing of the land surface occurs by solifluction and related periglacial processes, are

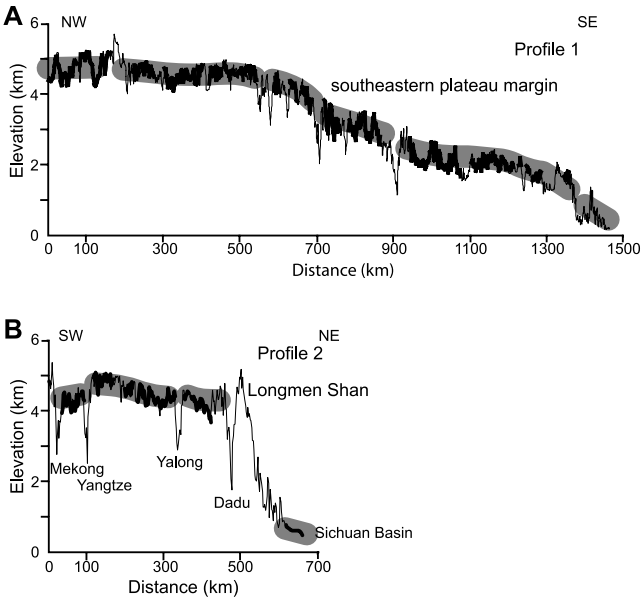

Figure 6. Topographic profiles. Actual topography along the profile is shown by the thin line. Thick line represents areas where remnant surfaces are preserved. Thick shading highlights surface patches and "patch-to-patch" continuity of surface remnants, where the width of this line represents the average local relief on the remnant surfaces. Profiles 1 and 2 are located parallel and perpendicular to the regional topographic gradient, respectively.

observed locally on the highest elevation remnant surfaces but generally occur within low-relief fluvial basins and do not appear to have significantly contributed to the relief on remnant surfaces.

[15] An example of the transition from relict to active landscape is shown for a tributary river to the Yalong River (a major tributary of the Yangtze River). Figure 7 shows a CORONA image and a longitudinal river profile over a total distance of ~200 km. The extent of the surface remnant is mapped by the contrast in albedo from moderately high values on the surface to low values in the deep river canyons, which was most easily seen on images with low Sun angles. The moderately high albedo area in the image shows the extent of the preserved remnant surface (Figure 7a). Where the river crosses this remnant surface it is a wide, braided alluvial stream with approximately 500 m of fluvial relief over a distance of about 100 km. The longitudinal profile shows a convexity that is coincident with a change in the river morphology from a wide valley with a braided alluvial river and flights of alluvial terraces to a narrower river valley with exposed bedrock walls and a narrow, boulder armor river bed (Figure 7d). Farther downstream, an abrupt knickpoint (abrupt change in slope of the river channel) is observed ~10 km before entering the main river and is associated with a steep channel slope and narrow channel and valley width.

[16] Low values of river steepness indices [*Kirby and Whipple*, 2001; *Wobus et al.*, 2006] and knickpoints separating alluvial rivers on high surfaces from bedrock reaches farther downstream were also used to distinguish the high surfaces from the active landscape [*Schoenbohm et al.*, 2004]. The low steepness values and alluvial character of the upstream portion of the tributary are associated with slow erosion rates (0.01–0.02 mm/yr) compared to the higher rates of erosion associated with the steep bedrock river valleys downstream (0.03–1 mm/yr), determined over both short and long timescales (10^4–10^6 years) [*Xu and Kamp*, 2000; *Ouimet et al.*, 2005; *Clark et al.*, 2005b]. Unmetamorphosed early Tertiary sediment and Eocene through Cretaceous low-temperature thermochronology ages [*Xu and Kamp*, 2000; *Clark et al.*, 2005b; *BGMRS*, 1990] suggest that less than 1 kilometer has been eroded from this surface since at least Eocene time (Figure 7 and Table 2). Average erosion rates of the remnant surfaces (~0.02 mm/yr) predict only ~200 m of erosion of since onset of rapid river incision at ~10 Ma, thus remnant

Table 1. Criteria for Remnant Surface Identification

	Description
Topography	locally, highest elevation in landscape
Longitudinal river profiles	channel segments with low steepness indices and knickpoints separating upstream alluviated channel reaches from bedrock channels downstream
Slope	moderately low slopes (between 1.2° and 10°)
Relief	low relief (<600 m)[a]
Geologic maps	lack of active sedimentation and limited (few hundred to several hundred meters) of mid to early Cenozoic sedimentation
Field observations	identification of slow weathering processes (i.e. hillslope creep and transport-limited (alluvial) rivers, periglacial or chemical weathering processes; saprolite/thick weathering profiles [*Schoenbohm et al.*, 2004]) that contrast with the active landscape (detachment-limited (bedrock) or mixed river channels, mass wasting, and debris flows)
CORONA imagery	moderately high albedo in images with low Sun angles; images are also used to evaluate relative elevation, slope/relief, and to identify active erosional processes from fluvial morphology and bed characteristics

[a]Some averaging of the relief across the remnant surface and active landscape occurs at the edges of the remnant surface. In these areas local relief can be as high as 1 km.

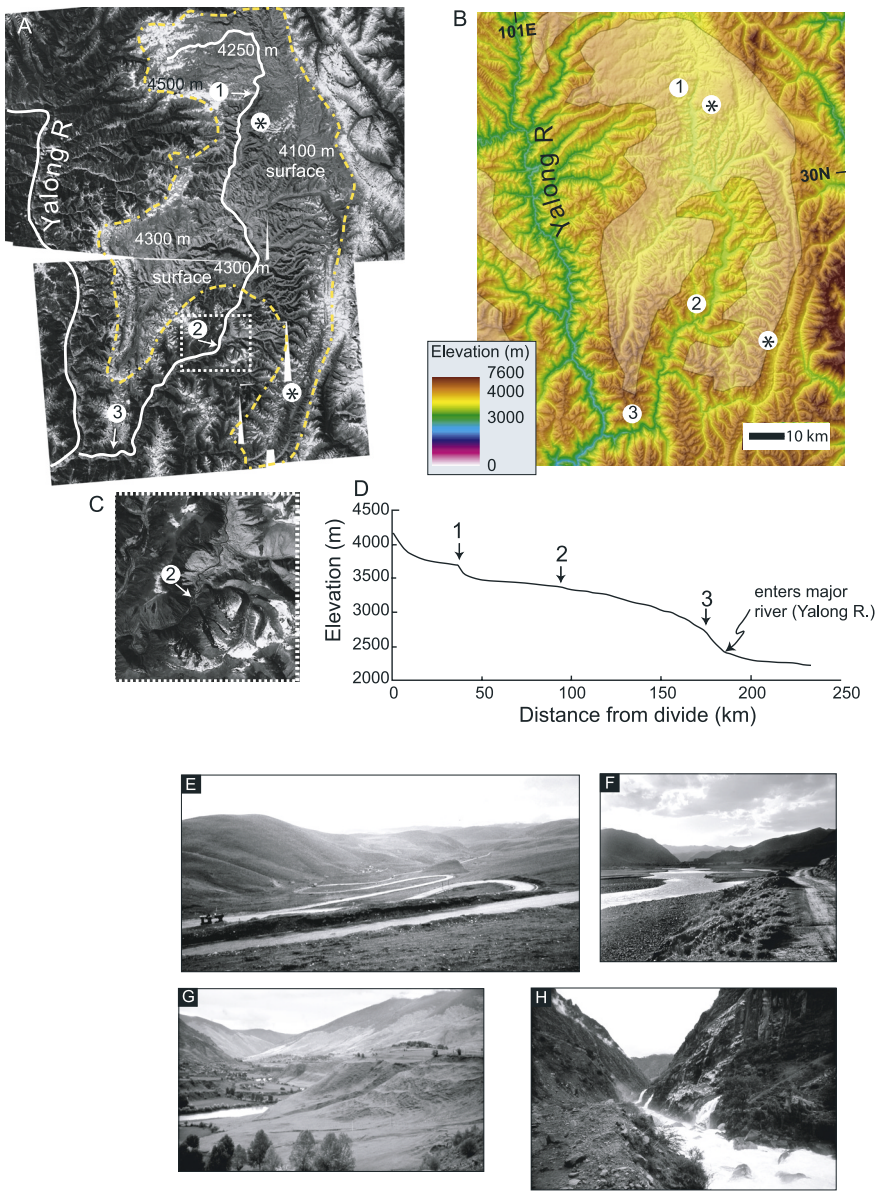

Figure 7. Example of fluvial transition from relict to active landscape. (a) Tributary to Yalong River (Li Qui River), which originates on a remnant surface (shown by moderately high albedo in the CORONA image) and flows across this remnant surface for ~100 km before it transitions into a deep river gorge before joining the Yalong River. Positions 1–3 on the map correspond to points on the river profile. (b) Digital topography for the same map extent as Figure 7a. (c) Close-up of river transition from relict to active landscape which is characterized by a wide, alluviated valley upstream and narrow river canyon downstream. (d) Elevation profile of Li Qui River. Positions 1–3 mark knickpoints (abrupt changes in river slope or concavity). Position 1 reflects the stream crossing a more resistant lithology (granite) compared to the surrounding Triassic metasediments (slates and quartzites). Position 2 marks a change in the river concavity from the upstream concave-up segment and the downstream concave-down segment. It is also associated with an abrupt change in river bed morphology from a wide, alluvial channel to a narrow bedrock/mixed channel. Position 3 is associated with an abrupt steepening of the channel just before it enters the mainstream (Yalong River). Star denotes locations of early Tertiary sedimentary rocks and thermochronology data that constrain minor erosion of the remnant surface in Cenozoic time. (e–g) Gradual changes in the river morphology along the portion of the channel that crosses the remnant surface. Figure 7g is located just above the transition in the river marked by position 2 in Figure 7a. It is associated with numerous fill and sediment-mantled strath terraces. Figure 7h is located on an adjacent tributary, equivalent to position 3 in Figure 7d, just before tributary joins the mainstream (Yalong River). This portion of the stream is deeply incised in a narrow river canyon and the bed is armored with coarse debris from numerous landslides [*Ouimet and Whipple*, 2004]. This portion of the river is considered to be the active landscape.

Table 2. Summary of Isotopic Ages Used to Interpret Age of Relict Landscape

Map ID	Reference	Method[a]	Age	Interpretation
1	*Arne et al.* [1997]	AFT	L. Miocene - E.Pliocene	rapid L Miocene - E. Pliocene cooling
2	*Arne et al.* [1997]	AFT	M. Jurassic	limited post M. Jurassic exhumation
3	*Arne et al.* [1997]	AFT	E. Jurassic	limited post E. Jurassic exhumation
4	*Arne et al.* [1997]	AFT	L. Miocene	rapid L. Miocene exhumation
5	*Arne et al.* [1997]	AFT	L. Miocene	rapid L. Miocene exhumation
6	*Arne et al.* [1997]	AFT	E. Cretaceous	limited post E. Cretaceous exhumation
7	*Arne et al.* [1997]	AFT	L. Paleocene - L. Eocene	limited post L. Eocene exhumation
8	*Arne et al.* [1997]	AFT	E. Cretaceous	limited post E. Cretaceous exhumation
9	*Arne et al.* [1997]	AFT	L. Cretaceous	limited post L. Cretaceous exhumation
10	*Arne et al.* [1997]	AFT	L. Cretaceous	limited post L. Cretaceous exhumation
11	*Arne et al.* [1997]	AFT	E. Oligocene	limited post E. Oligocene exhumation
12	*Clark et al.* [2005b]	AHe, AFT	L. Miocene	rapid L. Miocene exhumation
13	*Clark et al.* [2005b]	AHe	Jurassic - Eocene	slow Jurassic - Eocene exhumation
14	*Clark et al.* [2005b]	AHe	L. Miocene	rapid L. Miocene exhumation
15	*Huang et al.* [2003]	U-Th-Pb (mz), U/Pb (ti), Sm/Nd (gt), Rb/Sr (ms, bi)	E. Cretaceous - Olig.	slow E. Cretaceous - Oligocene cooling
16	*Kirby et al.* [2002]	AHe, AFT, ZrHe, K, $^{40}Ar/^{39}Ar$ (bi)	E. Jurassic - M. Miocene	slow E. Jurassic - M. Miocene cooling
17	*Kirby et al.* [2002]	AHe	E. Miocene	limited post E. Miocene exhumation
18	*Kirby et al.* [2002]	AHe, ZrHe, K, $^{40}Ar/^{39}Ar$ (bi)	E. Jurassic - M. Miocene	slow E. Jurassic - M. Miocene cooling
19	*Kirby et al.* [2002]	AHe	M. Miocene	limited post M. Miocene exhumation
20	*Kirby et al.* [2002]	AHe, ZrHe, K, $^{40}Ar/^{39}Ar$ (bi)	M. Jurassic - Pliocene	slow M. Jurassic - Miocene cooling, rapid L. Miocene cooling
21	*Kirby et al.* [2002], *Arne et al.* [1997]	AHe, AFT, ZrHe, K	L. Jurassic - L. Miocene	slow L. Jurassic - Miocene cooling, rapid M. Miocene cooling
22	*Niemi et al.* [2003, and references therein]	AHe, AFT, ZrFT, Rb/Sr (ms), K/Ar (bi), U/Pb (xt, mz, zr, ap)	Triassic - Eocene	slow Triassic-Eocene cooling
23	*Reid et al.* [2005b]	$^{40}Ar/^{39}Ar$ (bi, hb), U/Pb (zr)	L. Triassic	limited post late Triassic exhumation
24	*Reid et al.* [2005b]	$^{40}Ar/^{39}Ar$ (ms)	L. Triassic	limited post late Triassic exhumation
25	*Reid et al.* [2005b]	$^{40}Ar/^{39}Ar$ (bi), U/Pb (zr)	E. Cretaceous	limited post Cretaceous exhumation
26	*Reid et al.* [2005b]	$^{40}Ar/^{39}Ar$ (ms)	L. Triassic	limited post late Triassic exhumation
27	*Reid et al.* [2005b]	$^{40}Ar/^{39}Ar$ (bi, hb), U/Pb (zr)	L. Triassic	limited post late Triassic exhumation
28	*Reid et al.* [2005b]	$^{40}Ar/^{39}Ar$ (ms)	L. Triassic	limited post late Triassic exhumation
29	*Reid et al.* [2005b]	$^{40}Ar/^{39}Ar$ (ms)	L. Triassic	limited post late Triassic exhumation
30	*Reid et al.* [2005b]	$^{40}Ar/^{39}Ar$ (bi, hb), U/Pb (zr)	L. Triassic	limited post late Triassic exhumation
31	*Reid et al.* [2005b]	$^{40}Ar/^{39}Ar$ (bi), U/Pb (zr)	E. Cretaceous	limited post Cretaceous exhumation
32	*Wallis et al.* [2003]	$^{40}Ar/^{39}Ar$ (bi), U/Pb (ap)	Paleocene - Eocene	limited post late Eocene exhumation
33	*Wallis et al.* [2003]	$^{40}Ar/^{39}Ar$ (bi)	L. Cretaceous	limited post late Cretaceous exhumation
34	*Wallis et al.* [2003]	$^{40}Ar/^{39}Ar$ (bi, ms), U/Pb (zr)	Proterozic - M. Eocene	limited post late Cretaceous exhumation
35	*Wallis et al.* [2003]	$^{40}Ar/^{39}Ar$ (bi), U/Pb (zr)	E. Jurassic	limited post early Jurassic exhumation
36	*Wallis et al.* [2003]	$^{40}Ar/^{39}Ar$ (bi)	E. Jurassic	limited post early Jurassic exhumation

Table 2. (continued)

Map ID	Reference	Method[a]	Age	Interpretation
37	*Wallis et al.* [2003]	$^{40}Ar/^{39}Ar$ (ms, bi)	E. Cretaceous	limited post early Cretaceous exhumation
38	*Wallis et al.* [2003]	$^{40}Ar/^{39}Ar$ (ms, bi), U/Pb (zr)	E. Cretaceous	limited post early Cretaceous exhumation
39	*Wallis et al.* [2003]	$^{40}Ar/^{39}Ar$ (ms)	L. Miocene	rapid L. Miocene exhumation
40	*Xu and Kamp* [2000] (transect 1)	AFT, ZrFT	Permian - M. Miocene	slow late Permian - M. Miocene cooling/exhumation
41	*Xu and Kamp* [2000] (transect 2)	AFT, ZrFT	Permian - M. Miocene	slow late Permian - M. Miocene cooling/exhumation
42	*Xu and Kamp* [2000] (transect 3)	AFT, ZrFT	Permian - L. Miocene	slow late Permian - M. Miocene cooling/exhumation
43	*Xu and Kamp* [2000] (transect 4)	AFT, ZrFT	L. Triassic - Pliocene	slow L. Tr. - M. Mio. cooling/exh.; rapid Plio. cooling/exh at Gonga Shan
44	*Xu and Kamp* [2000] (transect 5)	AFT, ZrFT	M. Jurassic - Pliocene	slow M. Jur. - L. Mio. cooling/exh; rapid Plio. cooling/exh at Gonga Shan
45	*Xu and Kamp* [2000] (transect 6)	AFT, ZrFT	Permian - M. Miocene	slow L. Perm.- M. Mio. cooling/exh; rapid M. Mio. cooling/exh at Gonga Shan
46	*Xu and Kamp* [2000] (transect 7)	AFT, ZrFT	L. Paleocene - Pliocene	slow L. Paleo. - M. Mio cooling/exh; rapid Plio-Quat cooling/exh at Gonga Shan

[a]AHe, apatite (U-Th)/He; AFT, apatite fission track; ZrHe, zircon (U-Th)/He; ZrFT, zircon fission track; K, multiple diffusion domain modeling of K-feldspar $^{40}Ar/^{39}Ar$ spectra; mz, muscovite; ti, titanite; gt, garnet; bi, biotite; xt, xenotime; zr, zircon; ap, apatite; hb, hornblende.

surfaces do not appear to be strongly modified since canyon cutting began [*Clark et al.*, 2005b].

[17] Local relief and slope are key features of the remnant surfaces. The first-order feature of a relief map of the southeastern plateau is the contrast between the major river valleys (~1000–4200 m relief) and the high-elevation surfaces (<600 m relief) (Figure 8). Figure 9 shows an example of how the extent of remnant surfaces was determined from comparing different digital data sets. Areas that fit the high-elevation, low-slope and low-relief criteria of Table 1 are outlined in black. It was also important to demonstrate that the low-slope values that define the surface remnants were not primarily due to recent sedimentary deposition. Geologic maps show limited and local early Tertiary, Neogene and Quaternary sedimentary deposits throughout most of the eastern plateau [*BGMRS*, 1991; *Bureau of Geological and Mineral Resources of Yunnan Province* (*BGMRY*), 1990]. Extent and continuity of adjacent surface remnants were evaluated from viewing 3D topographic images (Figure 9e) and topographic cross-sectional profiles (Figure 6). Of particular importance is the ''patch-to-patch'' continuity of the surface from high to low elevation, and the concordant elevations across major river canyons (Figure 6). By combining all these criteria, we map the extent of the surface remnants in this area.

5. Description of Geology and Geomorphology of Remnant Surfaces by Region

[18] Descriptions of morphology and geologic history are used to summarize timing constraints on the evolution of this paleolandscape and its paleorelief. We divide the area into five provinces: (1) Songpan-Garze, (2) Longmen Shan and Yalong thrust belts, (3) Sichuan Basin, (4) South China Fold and Thrust Belts, and (5) Three Rivers fold and thrust belts (Figure 8). Local morphologic descriptions are a function of the geologic structure, tectonic history and lithology, as well as the elevation and climate history. Because Proterozoic to Mesozoic structures control much of the present-day crustal heterogeneity of the plateau, a discussion of each terrane begins with a brief summary of the predominant lithologies and salient structural history and is then followed by a description of the morphology. Both subsections integrate thermochronologic and stratigraphic data used to constrain the local age(s) of establishment, reworking and incision (abandonment) of the relict landscape.

5.1. Songpan-Garze Terrane

5.1.1. Geologic Summary

[19] Rocks of the Songpan-Garze terrane make up much of the high flat portion of the eastern plateau. They consist predominately of thick middle and upper Triassic flysch deposits that have been extensively folded, metamorphosed, and subjected to widespread postorogenic plutonism of latest Triassic to Jurassic age [*Mattauer et al.*, 1992; *Roger*, 1994; *Burchfiel et al.*, 1995; *Huang et al.*, 2003; *Harrowfield and Wilson*, 2005] (Figure 8). These plutons remain largely undeformed except by late Miocene–early Pliocene strike-slip faulting, indicating little post-Triassic contractional deformation consistent with structural evidence at the eastern and western margins of the terrane [*Wang et al.*, 1998; *Harrowfield and Wilson*, 2005; *Reid et al.*, 2005a] (Figure 10). The shallow pluton emplacement of 2.5 to 3 kb and preservation of Triassic shallow basin sediments in the eastern Songpan-Garze terrane limit the total post-Jurassic erosion to less than about 10 km [*Mattauer et al.*, 1992; *Roger*, 1994; *Burchfiel et al.*, 1995].

[20] Isotopic ages across the terrane indicate regional slow cooling and probably slow erosion (1–3°C/Myr) from

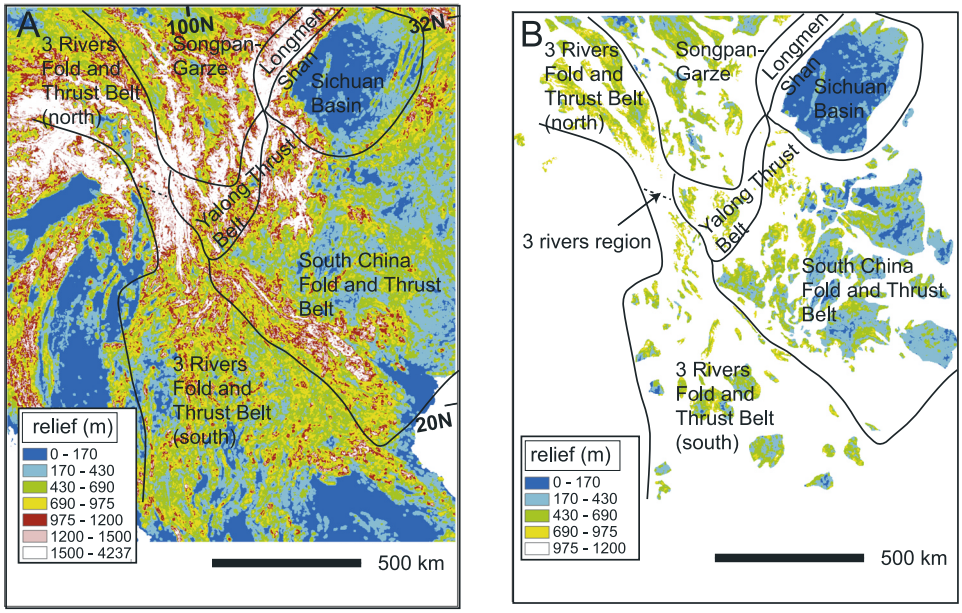

Figure 8. Relief maps derived from ~1 km digital topography calculated over a circular domain (radius = ~5 km). White represents areas where relief is >975 m. Tectonic terranes discussed in section 5 are outlined in black. (a) Relief values for the entire landscape. Areas of intense fluvial incision are characterized by high relief values (1000–4200 m). Low-relief areas (<600 m) correspond to headwater regions of tributary basins that have not yet adjusted to the incision rate set by the main river channels. (b) Map of relief values <975 m. Surface remnants correspond to regions with local relief <600 m, but some averaging of relief occurs between the edges of surface remnants and adjacent incised tributaries. This averaging at the margins of the remnant surfaces is associated with much higher relief (600–1000 m).

Jurassic time until at least Late Miocene time [*Kirby et al.*, 2002; *Niemi et al.*, 2003; *Huang et al.*, 2003; *Reid et al.*, 2005b] (Figure 10 and Table 2). Low-temperature thermochronology yields apparent exhumation rates between 0.01–0.02 mm/yr since Cretaceous time [*Xu and Kamp*, 2000; *Clark et al.*, 2005b]. However, the western Songpan-Garze terrane probably existed as a low-relief erosional highland because it has been a source of sediment in the Sichuan Basin since Jurassic time [*Burchfiel et al.*, 1995].

[21] Post-Triassic rocks are generally rare. Early Tertiary coarse clastic sedimentary rocks crop out in narrow fault-bounded basins that are associated with minor contractional deformation near the southern, southwestern and southeastern edges of the Songpan Garze flysch basin and adjacent terranes (Figure 10) [*BGMRS*, 1991]. These rocks are depositionally unconformable on an originally low-relief surface, and were modestly deformed by high-angle reverse faults and subsequently beveled to low relief. Deformed and undeformed Middle Miocene age granites are exposed in the southeast near the Gonga Shan massif [*Roger et al.*, 1995].

5.1.2. Surface Description

[22] Much of the Songpan-Garze terrane forms a high-elevation landscape with low-local relief (generally less than 600 m of relief at 4000–5000 m elevation) independent of lithology (Figures 7 and 8). River channels are alluvial where they flow across remnant surfaces and transition into steep, intensely incised bedrock canyons downstream as they join a major river or principal tributary. At elevations in excess of 4500 m, planar surfaces (< a few hundred meters of relief) are present across some of the granite plutons (Figure 5a). The formation of these more planar surfaces may be a combination of periglacial weathering processes acting on surfaces at high altitudes and the high susceptibility of particular granite compositions to chemical weathering. Alpine glaciation is locally observed, however the sedimentary and geomorphic record does not support the presence of widespread glacial erosion.

[23] Neogene and Quaternary sediments locally mantle surface remnants and are generally associated with active faults or are local fluvial and glacial deposits. These deposits limit the age of the low-relief surface to pre-Neogene, but the protracted period of slow cooling recorded by isotopic data and the limited amount of erosion since Jurassic time suggest that Songpan-Garze was a low-relief, slowly eroding landscape since Cretaceous time. Local early Tertiary contractional deformation suggests that some parts of the relict landscape were locally disrupted and then reestablished in early Cenozoic time.

[24] Recent structures and canyon cutting by major rivers disrupt remnant surfaces. Vertical displacement of remnant surfaces occurs across major active strike-slip faults of the Xianshuihe-Xiaojiang fault system and is less than the local relief of the relict surfaces (<600 m). The remnant landscape is locally disrupted by a few hundred meters by active normal faults that bound small graben (e.g., the Litang and Garze basins [*Wang et al.*, 1998]). These strike-slip and normal fault systems have been active since 8–4 Ma [*Wang et al.*, 1998]. Rapid unroofing of deformed and undeformed granites since 12 Ma in an area of high elevation and rugged terrain around Gonga Shan is evidence of remnant surface disruption [*Niemi et al.*, 2003; *Roger et al.*, 1995]. Rapid

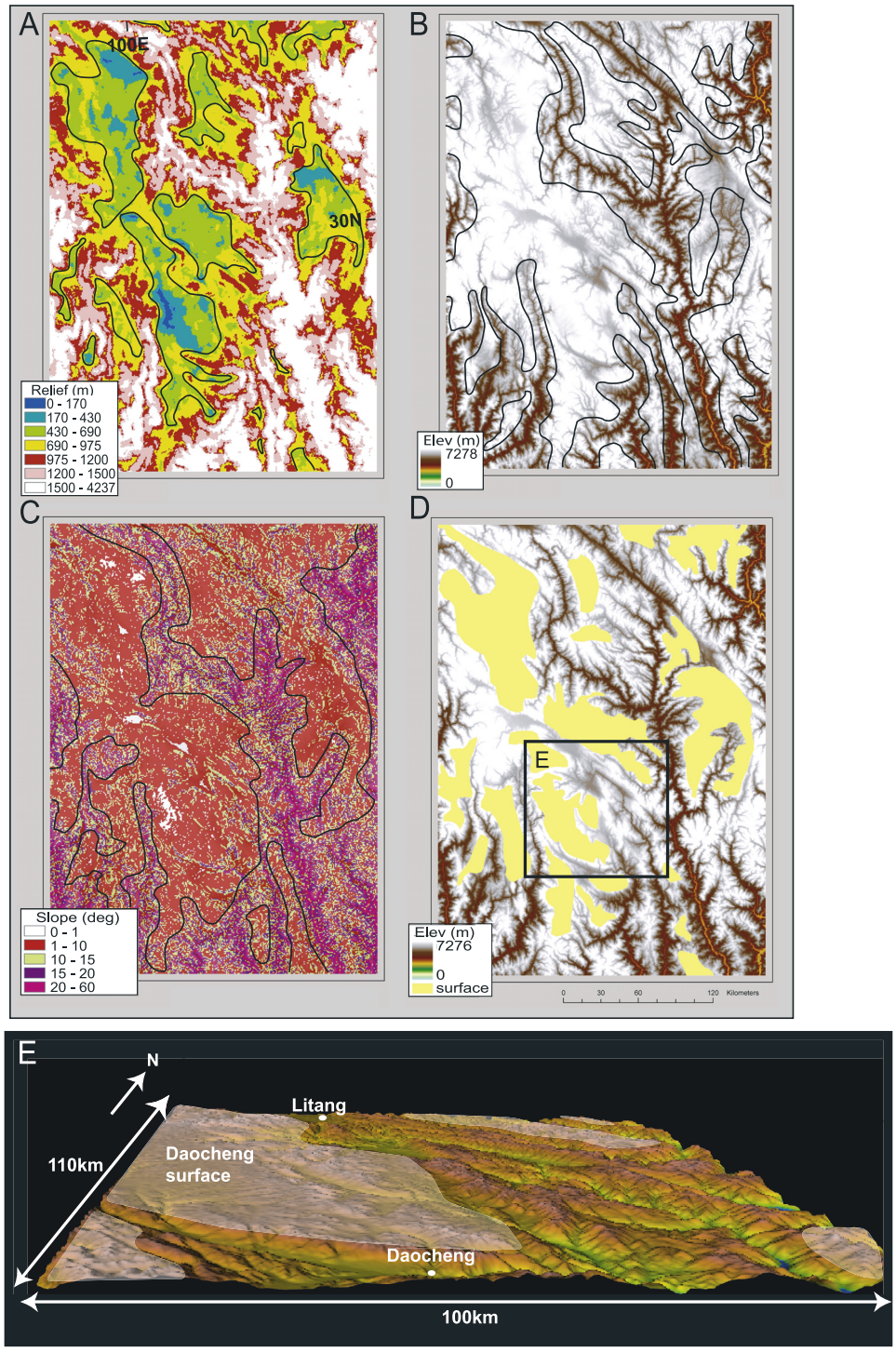

Figure 9. Example of surface characterization and identification from (a) relief, (b) elevation, (c) slope, and (d) map of remnant surfaces (yellow) determined from combining the data in Figures 9a–9c. Black outlines identify areas that meet criteria outlined in Table 1. (e) Example of 3-D image of digital topography, view to the north. Remnant surface areas are outlined in white on the left-hand side of the image and make up the highest elevation of the landscape (locally). Surface remnants are being actively destroyed by rapid river incision of the Yalong River and its tributaries in valleys shown on the right side.

erosion associated with canyon cutting of major rivers begins at 9–13 Ma [*Clark et al.*, 2005b]. Short-term (10^4–10^5 years) rates derived from stream sediment cosmogenic nuclide exposure ages (0.015–0.022 mm/yr on the relict landscape and 0.14–0.80 mm/yr in the Dadu River gorge [*Ouimet et al.*, 2005]) are in good agreement with long-term rates determined from low-temperature thermochronology elevation transects (0.02 mm/yr on the relict landscape and 0.25–0.5 in the river gorges [*Clark et al.*, 2005b]).

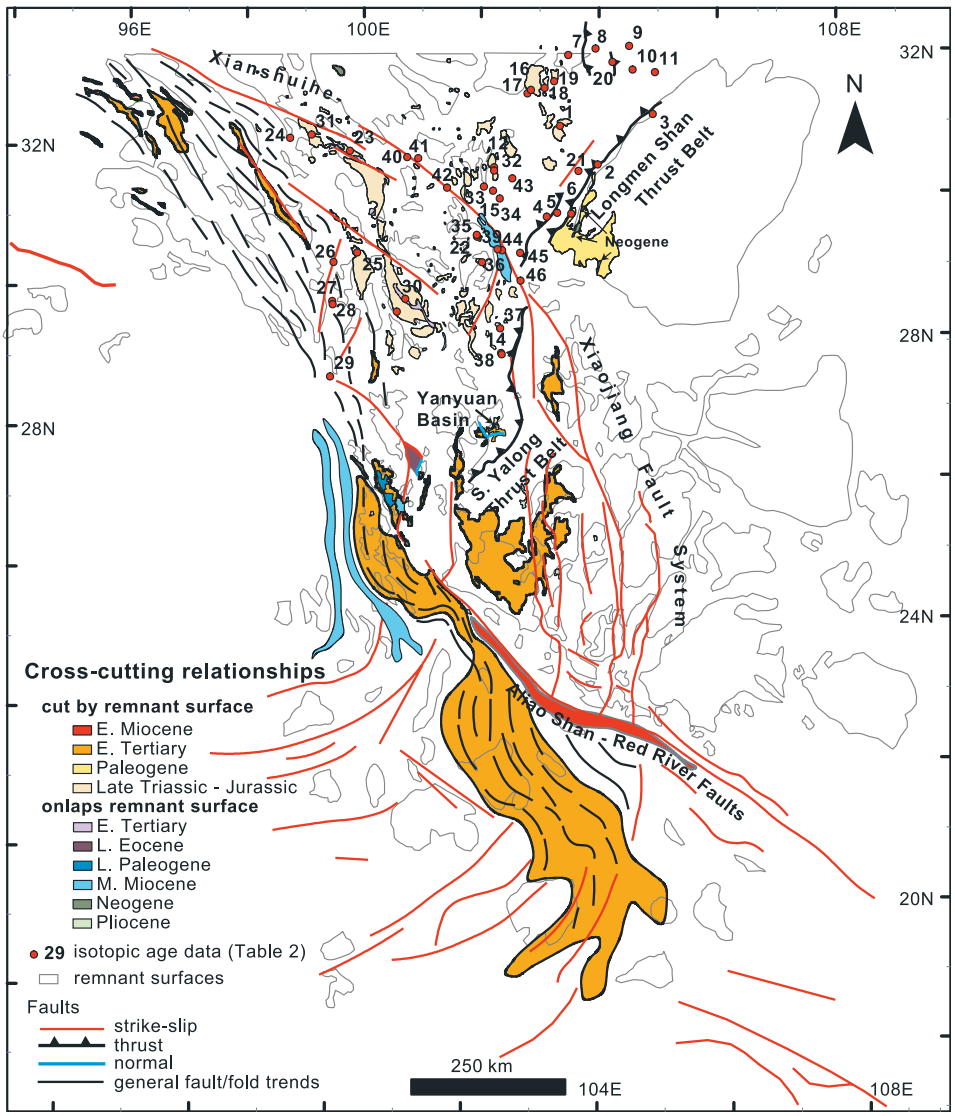

Figure 10. Map of crosscutting relationships that constrain age of relict landscape formation and abandonment. Warm colors represent rock units that are erosionally beveled by remnant surfaces (gray polygons). These units are a lower bound on the age of remnant surface formation. Cooler colors represent timing of deformation or deposition that affects remnant surfaces. These ages provide an upper bound on the age of the remnant landscape. Faults shown cut or disrupt remnant surfaces, with the exception of the generalized fold/fault trends shown for the Three Rivers Fold and Thrust Belt, which are cut by remnant surfaces (see discussion in section 5). Numbered point locations refer to isotopic data in Table 2. Only major units or outcrops are shown on this map. Numerous smaller, scattered outcrops of Tertiary sediment (especially in the South China Fold Belts) are not shown at this scale.

5.2. Longmen Shan and Yalong Thrust Belts

5.2.1. Geologic Summary

[25] The Longmen Shan and Yalong thrust belts define the southeastern boundary of the Songpan-Garze terrane and are composed of metamorphosed passive margin sedimentary sequences of Proterozoic through Paleozoic age and Proterozoic granitic basement rocks that were thrust eastward in late Triassic–early Jurassic time [*Mattauer et al.*, 1992; *Dirks et al.*, 1994; *Burchfiel et al.*, 1995; *Chen and Wilson*, 1996; *Wallis et al.*, 2003] (Figure 8). The Longmen Shan thrust belt was reactivated in Cenozoic time but Cenozoic shortening was probably limited to a few tens of kilometers [*Dirks et al.*, 1994; *Burchfiel et al.*, 1995]. Thermochronology suggests that rapid erosion related to forming the modern high elevation of the Longmen Shan did not develop until late Miocene time (~12–5 Ma) [*Kirby et al.*, 2002] (Figures 6 and 10 and Table 2). The Yalong thrust belt is the structural continuation of the Longmen Shan thrust belt across the Xianshuihe Fault. Cenozoic reactivation of the Yalong thrust belt involves Eocene rocks and may be contemporaneous with reactivation of the Longmen Shan thrust belt.

[26] A discontinuous, northeast trending belt of Cenozoic sediment is preserved between the northern and southern splays of the Yalong Thrust Belt [*BGMRS*, 1991; *BGMRY*, 1990] (Figure 10). Excluding the older, local depocenter of

the Jianchuan Basin proper, the oldest sediments in this belt are mapped as Eocene–Oligocene(?) (pre-Pliocene sediments in this belt do not have strict age control and their age designations should be considered as estimates, except in the Yanyuan Basin described next) and consist of fluvial sandstones, conglomerates and debris flows. They are flat lying to moderately folded or tilted, up to several hundred meters thick, and are distributed across an older low-relief landscape.

5.2.2. Surface Description

[27] The Longmen Shan thrust belt coincides with the trend of the steep plateau margin adjacent to the Sichuan Basin where the average elevation of the plateau margin is 4500 m with peak elevations between 6500–7500 m. No erosion surface remnants are preserved across this high-relief intensely dissected landscape (Figure 8). Alpine glacial erosion is active at elevations in excess of ~6000 m. The Yalong thrust belt trends subparallel to contours of constant elevation on the low-gradient slope of the southeastern plateau margin, but is not coincident with a steep topographic escarpment like the Longmen Shan. Remnants of a relict landscape are well preserved across the northern thrust splays and between its northern and southern splays. These remnants are disrupted in many, but not all, places by the southern splay of the Yalong thrust belt (Figure 10).

[28] Some parts of the Yalong thrust belt have experienced intense fluvial incision, especially along the Yalong River and its principal tributaries where local relief is up to 3 kilometers (Figure 8). Shallow gradient, alluvial rivers dominate the active erosion of remnant surfaces and transition downstream to become steep, narrow bedrock river gorges that eventually drain into the Yalong and Yangtze rivers. Glacial erosion is recognized at high elevations across the northern splay of the Yalong thrust belt.

[29] The age of surface remnants in the Yalong Thrust Belt are constrained by beveled, folded Eocene–Oligocene(?) rocks that are unconformably overlain by flat-lying Pliocene sedimentary rocks (Figure 10). In places, this sedimentary sequence contains multiple angular unconformities, and the folded Cenozoic sediments were deposited on a low-relief surface.

5.3. Yanyuan Basin

[30] The Yanyuan Basin is a Pliocene-Quaternary basin is located within the larger terrane of the Yalong Thrust Belt and is bounded to the south and west by active normal faults [*BGMRS*, 1991]. The basin surface forms a remnant surface and active normal faults that bound the west and southern edge of the basin offset this surface remnant by 300 m relative to correlative surface patches southwest of the basin. Here, early Eocene conglomerates, fluvial sandstones, volcaniclastics rocks and tuffs are deposited on an undulating karstic surface formed on folded Triassic rocks [*BGMRS*, 1991; *Si et al.*, 2000]. These sedimentary rocks are mapped as correlative with sandstones and conglomerates that crop out southwest of the basin and were deposited prior to the differentiation of the basin from the surrounding areas. These rocks experienced minor folding prior to deposition of flat-lying conglomerates of a similar lithology. The structurally highest sedimentary units have been eroded to low relief (Figure 5c). In the southern Yanyuan basin, fossiliferous, coal-bearing Pliocene sediments are deposited on an erosional surface of low-relief, limiting the latest age of erosional planation to pre-Pliocene [*BGMRS*, 1991; *Si et al.*, 2000] (Figure 10).

5.4. Sichuan Basin

5.4.1. Geologic Summary

[31] The Sichuan Basin is a part of the Yangtze platform that has largely escaped the deformation of different ages that has affected the surrounding regions (Figures 2 and 8). The Sichuan Basin contains a thick section of Upper Triassic to Cretaceous foredeep sedimentary rocks deposited in response to Mesozoic thrusting in the north and northwest [*Chen et al.*, 1995; *Burchfiel et al.*, 1995; *Li et al.*, 2003; *Meng et al.*, 2005]. Isolated outcrops of folded Paleogene sedimentary rocks are present in the southwest corner of the basin and the adjacent foothills and are capped by thin, locally deposited Neogene sedimentary rocks [*Burchfiel et al.*, 1995] (Figure 10). Pre-Neogene rocks within the Sichuan Basin (500 m asl) are stratigraphically continuous with deposits east and south of the basin, that lie at modern elevations of 2–3 km. The Sichuan Basin lacks a Cenozoic foredeep, despite reactivation of thrusting and development of high topography in the Longmen Shan during this time [*Burchfiel et al.*, 1995; *Royden et al.*, 1997; *Kirby et al.*, 2002]. Only a thin veneer of <200 m of alluvial Quaternary sediment is preserved in the southwestern part of the basin [*BGMRS*, 1991]. The southwestern portion of the basin is being actively shortened but rates are slow [*Burchfiel et al.*, 1995]. The Quaternary strata, as well as the rest of the rocks of the basin, are being actively incised.

[32] Seismic tomography indicates that the Sichuan Basin is underlain by a fast seismic anomaly, extending at least to 250 km depth, suggesting that the lack of deformation of the Sichuan Basin may be attributed or related to the presence of a thick, cold mantle root [*Lebedev and Nolet*, 2003]. The Sichuan Basin also has relatively low heat flow (40–70 mW/m^2) compared to the adjacent elevated region of the southeastern plateau margin (60–100 mW/m^2) [*Hu et al.*, 2000].

5.4.2. Surface Description

[33] The subdued relief of the Sichuan Basin cannot be attributed to Cenozoic sedimentary deposition (Figure 8). Modern sediment derived from the Longmen Shan bypasses the Sichuan Basin and is carried to the southeast into the Yangtze River. Detrital apatite fission track ages from Mesozoic sedimentary rocks are similar to their depositional age, limiting the amount of burial and subsequent erosion to less than a few kilometers since Cretaceous time [*Arne et al.*, 1997] (Table 2). However, we cannot be certain of negligible erosion of the Sichuan Basin because AFT borehole data from northwestern Sichuan Basin [*Xu*, 1997] and a single surface detrital sample [*Arne et al.*, 1997] are interpreted to indicate 2–3 km of Neogene denudation [*Xu and Kamp*, 2000]. Eocene to Cretaceous apatite and zircon fission track ages from high elevations within the Songpan-Garze terrane west of the Longmen Shan [*Xu and Kamp*, 2000] (Table 2) suggest that erosion surface remnants preserved across the Songpan-Garze terrane may be correlative with the low-relief landscape of the Sichuan Basin, in the case of minimal burial and exhumation of the basin during Late Cenozoic time. If so, then the

~4 km offset of the remnant surfaces between the plateau and the Sichuan Basin represents a maximum vertical offset across the Longmen Shan. Erosion surface remnants preserved to the south in the South China Fold Belts at 1–3 km modern elevation may also correlate with the landscape surface of the Sichuan Basin where recent vertical offset of surface remnants is accommodated by steep, post-Paleogene faults bounding the south side of the basin.

5.5. South China Fold Belts

5.5.1. Geologic Summary

[34] The South China Fold Belts refers to a structurally and lithologically diverse area that is south and southeast of the Sichuan Basin and Yalong Thrust Belt and northeast of the Three Rivers Fold and Thrust Belt, which includes the southern Yangtze Platform (in a strict sense) [*Wang et al.*, 1998] (Figure 8). Proterozoic and Paleozoic sedimentary rocks are exposed in the east, and underlie thick Mesozoic (locally Paleogene) sedimentary basins in the west (the Chuxiong Basin and the Daliang Basin). Proterozoic metamorphic and granitic basement rocks outcrop locally [*BGMRS*, 1991; *BGMRY*, 1990]. In the south, flat-lying Eocene sedimentary rocks have been deposited on folded Triassic–Proterozoic rocks over a low-relief karst surface [*Wang et al.*, 1998]. Folding of Paleozoic–Eocene, rarely Oligocene, rocks occurs in the Chuxiong and Daliang basins and may be contemporaneous with Cenozoic reactivation of the Yalong Fold and Thrust Belt [*Leloup et al.*, 1995; *Wang et al.*, 1998]. Outcrops of mapped Paleogene strata are scattered and quite numerous across the South China Fold Belts, making it difficult to say how strong or extensive the early to middle Cenozoic deformation may have been. Upper Oligocene–Miocene rocks are generally absent. Folds involving Paleogene rocks are erosionally beveled and locally unconformably overlain by flat-lying, coal bearing Pliocene, rarely uppermost Miocene–Pliocene, sedimentary rocks (Figure 10).

5.5.2. Surface Description

[35] Commonly referred to as the "Yunnan Plateau," the region of the South China Fold Belt ranges in elevation from ~3 km in the northwest to less than <1 km in the southeast where the relict landscape dips southeastward and merges with the coastal plain (Figures 2, 3, and 8). Remnant erosion surfaces are well preserved across most of the area, disrupted by a few hundred meters only in areas of local active faulting [*Wang et al.*, 1998; *Schoenbohm et al.*, 2004] and by limited fluvial incision. The modern climate in the South China Fold Belt is more humid than areas to the north and modern karst topography and thick saprolite and soils are common (Figure 5d).

[36] The remnant surfaces of the South China Fold Belt are cut by deep river gorges only along the Yangtze, Pearl and Red Rivers, and much of the deep incision is limited to the main rivers and short reaches on lower principal tributaries. This area is less incised than the Yalong Thrust Belt and the Songpan-Garze terranes, probably because of its lower modern elevation.

[37] Surface remnant morphology is distinct on slope maps, showing a sharp transition from low slope areas of the remnant surfaces to high slope areas that are intensely fluvially dissected and contain steep, narrow canyons. However, along some tributaries to major river systems in the South China Fold Belt and segments of the Yangtze River, narrow river canyon walls have not been maintained and rapidly incising rivers have developed broad river valleys, whose main lower channel becomes alluviated and the steep bedrock reaches are spatially limited to a short reaches where the river first flows across the edge of a remnant surface. This fluvial incision pattern is common in the areas of the Chuxong Basin and the Daliang Basin and probably occurs because the Mesozoic–Tertiary sedimentary rocks are easily eroded. The wide alluviated river bottoms have very low slope values (less than 1.2°) so that remnant surfaces are difficult to identify from a slope map alone.

[38] The initial ages of the remnant surfaces may be diachronous across this region. Flat-lying Eocene sedimentary rocks limit the age of the surface to Eocene or older in the south [*Wang et al.*, 1998]. Numerous belts of mapped Paleogene strata have been both strongly and weakly folded. Where present, remnant surfaces cut across deformed rocks as young as Paleogene and are onlapped by local Pliocene sedimentary rocks, limiting the age of the latest erosional planation to post-Paleogene. Pliocene–Quaternary graben vertically offset the surface remnants, but most of the strike-slip faults in this area do not, except for the Xianshuihe Fault in the northern Anning River valley. Vertical offset across this fault is ~1–1.5 km near the headwaters of the Anning River and decreases to the south where the offset disappears. This surface offset occurs in the local area of high elevation and rapid denudation since 12 Ma near the Gonga Shan massif (7756 m) [*Roger et al.*, 1995; *Niemi et al.*, 2003] (Figure 5f).

5.6. Three Rivers Fold and Thrust Belt

5.6.1. Geologic Summary

[39] The Three Rivers fold and thrust belt (TRFB) is a complex region of small, continental fragments and arc terranes accreted in late Paleozoic through Mesozoic time including eastern portions of the Lhasa Block, Qiantang Block, Yidun Arc and their counterparts further south (Figure 8). Many of the Paleozoic and Mesozoic suture zones and tectonic boundaries in this region were reactivated during Cenozoic time and Cenozoic deformation has affected all of the TRFB. Erosionally beveled, fault bounded Paleogene sedimentary basins in the north were probably coeval with Paleocene–Eocene shortening deformation documented in the east central plateau, where total denudation and shortening during this time was minimal [*Horton et al.*, 2002]. In the south, Cenozoic deformation appears to have been accommodated by shortening, strike-slip faulting, and clockwise rotation of small crustal fragments in a complicated manner [*Wang and Burchfiel*, 1997]. The left-lateral transpressional Ailao Shan Shear Zone is the principal boundary separating the intensely rotated and deformed region of the Three Rivers fold and thrust belt to the southwest from the less deformed South China Fold Belt. Cooling ages from the shear zone suggest that deformation occurred between 34 and 17 Ma [*Leloup et al.*, 1995, 2001; *Gilley et al.*, 2003] and may be contemporaneous with thin-skinned folding and thrusting of Mesozoic–early Tertiary sediments of the Lanping-Simao Basin and the Qiantang Block [*Wang and Burchfiel*, 1997] (Figure 10).

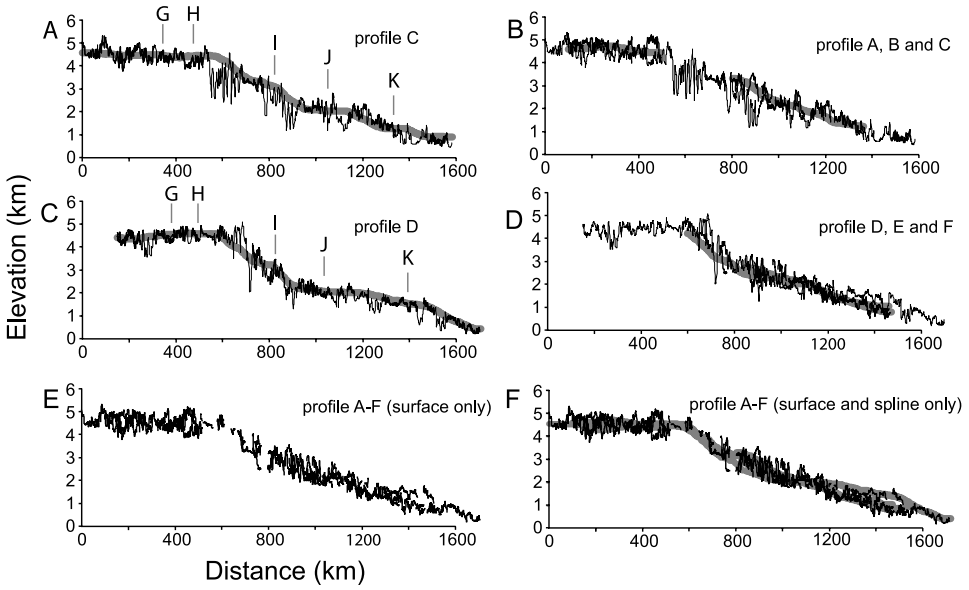

Figure 11. Topographic profiles parallel to regional topographic gradient. Locations of profiles are shown in Figure 3. Actual topography along the profile is shown by the thin solid line. Thick solid line represents areas where remnant surfaces are preserved. Thick shaded line shows elevation of interpolated fit (spline) to remnant surfaces, where the width of this line represents the average local relief on the remnant surfaces. (a) Profile C with remnant surfaces and interpolated (spline) fit. Letters G–K show locations of the intersecting cross profiles in Figure 12. (b) Remnant surfaces and spline fits from profiles A and B projected onto actual topography of long profile C. (c) Long profile D with actual topography, remnant surfaces and spline fit. Letters G–K show locations of the intersecting cross profiles in Figure 12. (d) Remnant surfaces and spline fit for profiles E and F projected onto the actual topography of profile D. (e) Remnant surfaces for all profiles projected onto line of Profile C. (f) Remnant surfaces and spline fits for all profiles projected onto line of Profile C.

5.6.2. Surface Description

[40] The TRFB occurs beneath the topographically high flat plateau and beneath the gently sloping southeastern plateau margin to low elevations (Figure 6). The paleolandscape surface that mantles the southeastern plateau forms a smooth carapace across much of the Three Rivers Fold and Thrust Belt and the adjacent tectonic boundaries (Figures 2, 3, 11, and 12). Some of the TRFB has locally high mountains that indicate some local conditions of young faulting.

[41] Much of the Three Rivers fold belt has been eroded to low local relief, including the mid-Tertiary Aliao Shan Shear Zone [*Schoenbohm et al.*, 2004]. In the Lanping-Simao belt, rocks deformed after the early Tertiary were beveled by erosion and then covered unconformably by onlap of Pliocene sediments [*BGMRY*, 1990]. West and south of the Lanping-Simao Basin, remnant surfaces are commonly preserved on top of fault blocks that have been rotated and more intensely dissected, resulting in a greater degree of disruption of the remnant surfaces than is seen elsewhere. This reflects the intensity of Cenozoic deformation in this area, which is mostly strike-slip faulting that does not produce significant topographic relief. However, erosion that occurs in response to this deformation has not been significant enough to completely destroy surface remnants. Also, the average elevation of surface remnants in this region is similar to much less deformed areas to the east in the South China Fold and Thrust Belt.

[42] No remnant surfaces are observed in the Three Rivers region, which is an area of intense dissection and high relief (~1000–4200 m) covering an area roughly 100 km by 300 km and is a locus of strike-slip and compressional deformation which ended by middle Miocene time [*Akciz et al.*, 2001; *Akciz*, 2004; *Hallet and Molnar*, 2001; *Clark et al.*, 2004] (Figure 8). North and south of this area, remnant landscape surfaces are well preserved in between the Salween, Mekong, and Yangtze rivers.

5.7. Late Miocene to Recent Tectonic Activity

[43] Throughout all five provinces, the recent geologic record is dominated by strike-slip faulting, consistent with the modern-day strain field determined from GPS data [*King et al.*, 1997; *Chen et al.*, 2000; *Wang et al.*, 1998]. Graben-style normal faults are common and associated with the transfer of motion between individual strike-slip fault segments. Remnant surfaces are generally not vertically offset by strike-slip faults except in a few places where discrete offsets can be measured from preservation of remnant surfaces within individual fault blocks. This deformation pattern accommodates rotation of crustal fragments around the eastern Himalayan syntaxis without significant translation of upper crustal material toward the eastern foreland [*King et al.*, 1997; *Chen et al.*, 2000; *Wang et al.*, 1998]. Taken together, these data along with the absence of late Miocene–Pliocene shortening structures suggest that surface shortening perpendicular to the topographic

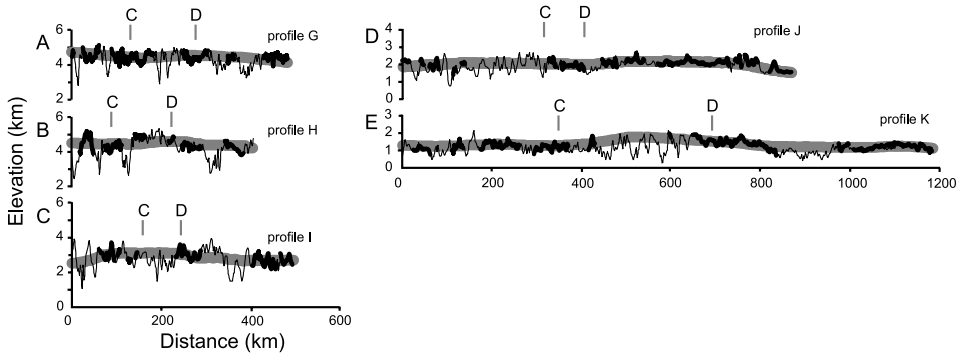

Figure 12. (a–e) Topographic profiles perpendicular to regional topographic gradient. Locations of profiles are shown in Figure 3. Actual topography along the profile is shown by the thin solid line. Thick solid line represents areas where remnant surfaces are preserved. Thick shaded line shows elevation of interpolated fit (spline) to remnant surfaces, where the width of this line represents the average local relief on the remnant surfaces. Letters C and D show location of intersecting parallel profiles from Figure 11.

gradient has been minor since at least Miocene–Pliocene time, consistent with the regional preservation of remnant surfaces.

6. Reconstruction of a Relict, Low-Relief Landscape From Surface Remnants

[44] The regional continuity of remnant surfaces, and their lack of correlation to a particular lithology or tectonic province, are used to test the hypothesis that these surfaces collectively comprise a paleolandscape. Remnant surfaces are then used to interpolate a smooth surface that represents the modern altitude of the reconstructed relict landscape. Finally, we calculate the vertical displacement of the relict landscape by subtracting an assumed initial elevation from its modern altitude.

[45] Remnant surfaces are observed in all five tectonic provinces, although local characteristics vary as a function of bedrock lithology, degree of Cenozoic deformation and relative latitude and altitude. Several topographic profiles taken parallel to the regional topographic gradient show that the individual surface remnants, over a distance of >1000 km, are observed at 5 km to <1 km asl where they merge with the coastal plain of the South Asian marginal seas (Figure 11). We observe that the offset between adjacent remnants is within the amount of local relief observed on the surfaces themselves (<600 m). Profiles taken perpendicular to the regional topographic gradient, also demonstrate the regularity in the altitude of adjacent remnants (Figure 12). Although the relict landscape has been locally disrupted by active faulting, tectonic deformation has not played a significant role in the disruption or destruction of the eastern plateau relict landscape with two exceptions. Surface remnants have been offset a maximum of 3–4 km across the Longmen Shan due to largely vertical motion concentrated along this steep plateau margin [*Kirby et al.*, 2002, 2003]. Also, a discrete (vertical) offset of 1–1.5 km occurs across the left-lateral Xianshuihe fault, but only in the vicinity of the Anning River (Figures 1 and 3). This vertical offset decreases from north (the headwaters of the Anning River) to south, where it eventually disappears just west of the southern splay of the Yalong Thrust Belt.

[46] Another measure of the continuity of remnant surfaces is the fluvial network, which is continuous across both active and relict elements in the landscape. That is, streams originate on remnant surfaces and transform downstream to become part of the active landscape. Although there is evidence for large-scale drainage reorganization by river capture and reversal [*Clark et al.*, 2004, and references therein], reorganization has not caused hydrologic isolation of surface remnants, in which case surface remnants could have eroded to a different base level, and elevation, than the surrounding area. Also, comparison of channel parameters to local relief suggests that the low local relief morphology is due to fluvial erosion processes. Using typical average parameters for steepness (k) and concavity (θ) ($k_{sn} = 60–90$ are typical values for a reference concavity of $\theta = 0.45$) measured for channel profile segments on the relict landscape [*Kirby et al.*, 2003; *Schoenbohm et al.*, 2004], we estimate the fluvial relief (the elevation gain along a channel profile) to be $R_f = \sim 600$ m for channel lengths of 5 km [*Whipple and Tucker*, 1999, equation (22a)]. This relief estimate is consistent with the relief of the remnant surfaces ($R < 600$ m), averaged over a circular area with radius $\sim$ 5 km. Thus local relief values determined from digital topography are consistent with the fluvial relief calculated from channel parameters determined from the longitudinal stream profiles. Hydrologic continuity of adjacent remnants and a fluvial origin of the low-relief morphology implies that surfaces were mutually graded to the major rivers and probably eroded to a similar elevation as the surrounding area during their formation.

[47] Using the geographic extent and modern altitude of surface remnants, we fit an interpolated surface through the remnant patches to define a reconstructed relict landscape. The interpolated surface was determined using a spline interpolation (with tension) and solving for best fit parameters for the remnant surfaces across the plateau margin (Figure 13a). This provides a smooth surface that fits the topography of the remnant surfaces within the relief of the surfaces themselves, typically ±300 m. Plotting the spline surface and topography along down-slope and cross-slope sections shows that the spline provides an acceptable fit to the individual remnant surfaces (Figure 11 and 12). Sub-

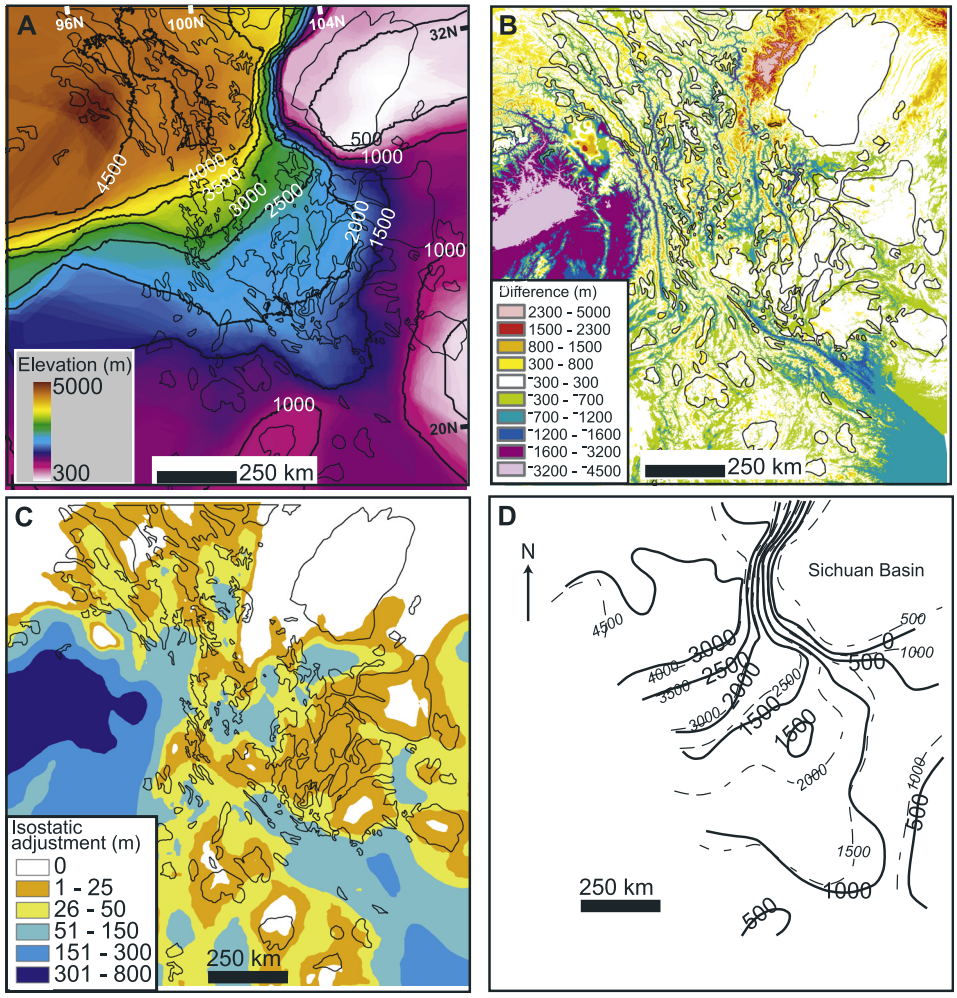

Figure 13. Topography modeling from remnant surface data. (a) Interpolated (spline) fit to remnant surfaces colored by elevation with 500 m elevation contours. Locations of remnant surfaces are shown by black polygons. This interpolated surface represents the reconstructed relict landscape that has been warped and elevated in response to crustal thickening. Spline values outside region with remnant surfaces are meaningless (i.e., in the region of the eastern Himalayan syntaxis). (b) Deviations of actual elevation from interpolated spline surface in Figure 13a. Negative values are associated with actual elevations that lie below the spline surface. Regions of high negative values (incision into the relict landscape) correspond to deep, narrow gorges of the major rivers. Positive values represent areas where the actual elevation is higher than the spline surface. These regions correspond to resistant lithologies, recent structural activity, and focused deformation adjacent to the Sichuan Basin (Longmen Shan). (c) Calculated isostatic adjustment due to erosion. (d) Calculated vertical displacement map shown by 500 m contours. Thick solid line and dashed line represent minimum and maximum estimates, respectively, based on a range of calculated paleoslopes between 10^{-3} and 10^{-4}.

traction of the observed topography from the spline surface and masking values within the local relief of remnant surfaces (±300 m) shows that few areas within the surface remnants are not fit by the spine surface (Figure 13b).

[48] The interpolated surface is smoothly varying across the variable orientations of the tectonic terranes. There is little correlation of the orientation or offset of the interpolated surface with major surface structures except for the aforementioned structures in the Longmen Shan and Yalong thrust belts.

[49] Slow long-term erosion rates of the remnant surfaces allow us to use the modern elevation of the relict landscape as a measure of long-term vertical deformation. We calculate the vertical displacement by subtracting the initial elevation of the relict landscape from its modern altitude. We assume the original regional paleogradient of the relict landscape to be between 10^{-3} and 10^{-4}, consistent with modern regional-scale, low-relief river basins such as the Mississippi and Amazon drainage basins. The fact that the relict landscape merges with the modern coastal plain indicates that the paleo-base level was at sea level. For simplicity, we assume that the regional paleoslope was southeast, given by the general drainage direction of the major rivers, with a constant slope between 10^{-3} and 10^{-4}

and zero elevation at the modern coastline. We calculate a maximum and minimum elevation change based on the range of paleoslope estimates, suggesting that the highest parts of the southeastern plateau have been elevated in excess of 3–4 km (Figure 13d). The contours of vertical displacement are parallel to both the slope of the assumed paleogradient and the modern topography. If we assume a different orientation for the paleogradient, the displacement contours will shift orientation and/or in magnitude. However, because the assumed paleogradient is small compared to the modern elevation of the relict landscape, the effect is minor.

[50] The vertical displacement of the relict landscape is the sum of underlying tectonic processes, which we assume to be related to crustal thickening, and isostatic compensation due to surface erosion. If erosion is spatially limited to major river gorges, we may expect that evacuation of material from these rivers may contribute an increase in the elevation of the much less eroded relict landscape due to isostatic rebound [e.g., *Whipple et al.*, 1999]. We can estimate the effect of isostatic adjustment from the magnitude of erosion calculated from the difference in observed topography and the spline fit (excluding the areas of remnant surfaces). Erosion was spatially averaged to a length scale over which crustal loads might reasonably be compensated (flexural wavelength = 100 km), considering that the flexural strength of the crust for the plateau is quite low (Te = 10 km) [*Masek et al.*, 1994; *Jordan and Watts*, 2005]. Larger values of flexural wavelength and higher strength produce smaller values of isostatic rebound. Therefore we suggest that our chosen parameters give an upper limit on the amount of isostatic adjustment. The resulting map shows that the maximum contribution to the modern topography from isostatic adjustment due to surface erosion, excluding the Longmen Shan region, is generally less than 50 m across much of the southeastern plateau margin and might be as much as 150 m in regions that are more extensively dissected (Figure 13c). This value is small compared to the calculated vertical displacement and suggests that almost all of modern elevation of the relict landscape is due to crustal thickening (Figure 4).

7. Landscape Evolution: The Age of the Relict and Active Landscapes

[51] The diachroneity of erosion and sedimentation processes that formed the relict landscape of the eastern Tibetan Plateau is evident in the sedimentary and geomorphic record (Figure 10). Some areas of the remnant surfaces have not experienced deformation or erosion since Eocene or Cretaceous time while others show clear evidence for early Tertiary deformation followed by (re)development of the low-relief landscape (Figure 14). The former can be demonstrated in areas where flat-lying or gently deformed Eocene sediments unconformably overlay older deformed rocks, or where isotopic data indicate limited or slow erosion since Late Cretaceous time. The latter is demonstrated in areas where Paleogene sediments have been deposited, deformed, and subsequently eroded to elevations conformable with the surrounding landscape. Locally, unconformities developed above deformed and beveled sedimentary rocks of early Tertiary age are onlapped by undeformed, flat-lying Pliocene and rarely, upper Miocene sediments. Thus the relict landscape is a dynamic feature with a complex history of development, local disruption and reestablishment of the low-relief landscape. Sedimentary and structural relationships suggest that this complex history of the low-relief landscape history, including local deformation and subsequent redevelopment, largely occurred prior to deep incision of the modern river system into the relict landscape.

[52] Isotopic ages and the general absence of metamorphism or ductile deformation in Mesozoic and Cenozoic age sedimentary rocks suggest that the exhumation level of the southeastern plateau margin is not greater than a few to several kilometers, with the exception of localized, narrow deformation belts in the Ailao Shan Shear Zone (ASSZ), Yulong-Snow Mountains, Gonga Shan massif, and the Chongshan and Gaoligong shear zones [*Roger et al.*, 1995; *Leloup et al.*, 1995; *Lacassin et al.*, 1996; *Leloup et al.*, 2001; *Gilley et al.*, 2003; *Niemi et al.*, 2003; *Akciz*, 2004]. Therefore we propose that much of the regional low-relief character of the relict landscape was not associated with significant erosion of formerly high-relief, high-elevation topography. For example, many Mesozoic to early Tertiary sedimentary basins occur across eastern plateau; these were deformed into broad fold belts without evidence for deep level erosion commonly associated with high, mountainous topography. Sedimentary basin formation, followed by moderate deformation that did not create steep or laterally extensive high topography, suggests that the formation of the relict landscape did not involve extensive, rapid early Cenozoic planation to produce a regionally low-relief, low-elevation paleolandscape.

[53] A variety of data suggest that the elevated remnants of the relict landscape are now undergoing rapid destruction by bedrock erosion of major rivers that drain the eastern Tibetan Plateau. Data from apatite (U-Th)/He and fission track thermochronology show that bedrock river incision began by 9–13 Ma [*Clark et al.*, 2005b], coincident with development of the steep Longmen Shan margin [*Kirby et al.*, 2002]. River incision must necessarily postdate the uplift of the relict landscape to its modern altitude because it would be impossible to form deep bedrock rivers into a low-elevation landscape. These data, by themselves, cannot determine if the initiation of rapid bedrock incision was coeval with an increase in surface elevation or if there was a significant lag time before the onset of rapid incision. Whereas a lag time that would be significant in comparison to the uncertainty of our estimate of the onset of rapid cooling due to river incision (±2 Myr) is plausible, it seems rather unlikely.

[54] The transient condition of the landscape suggests that the landscape response time is greater than ~10 Ma. There may be several factors that contribute to the preservation of remnant surfaces, and to the long landscape response time in this area. Knickpoints that separate relict from active landscape, may be propagating slowly, particularly into areas of rapidly decreasing drainage area. Some knickpoints may not be migrating at all, and may be stationary due to resistant lithology, bed armoring by landslide debris [*Ouimet and Whipple*, 2004] or spatial variations in fault motion. Stationary knickpoints may arrest or retard the propagation of new erosional conditions and effectively

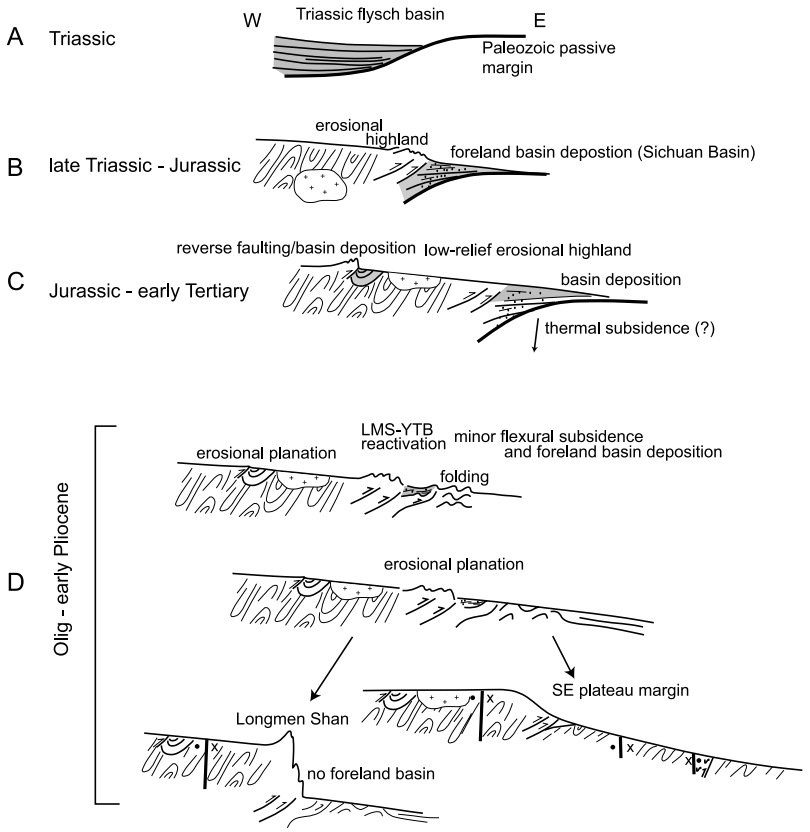

Figure 14. Schematic diagram of geologic/topographic evolution of the southeastern Tibetan Plateau. (a) Triassic time. Following deposition of a passive margin sequence followed by continental rifting in late Paleozoic time, deposition of a broad, deep-water (flysch) basin occurs in Triassic time in the area that will become the high elevation eastern plateau (Songpan Garze flysch). (b) Transpressional margin develops and flysch deposits are extensively folded in late Triassic time, followed by widespread, postorogenic plutonism in late Triassic–Jurassic time. Initiation of the Longmen Shan thrust belt and foreland basin deposition in the Sichuan Basin occurs in latest Triassic-Jurassic time. (c) Songpan Garze terrane continues to be a source of sediment to the Sichuan Basin from Jurassic–early Tertiary time, but total magnitude of post-Jurassic erosion is limited to <10 km. The Songpan Garze terrane likely existed as a low-relief erosional highland during this time. High-angle reverse faulting and local basin deposition occurs in early Tertiary time within the western Songpan Garze terrane, but total horizontal shortening is not significant. Undeformed late Triassic plutons also indicate little post-Triassic deformation of the Songpan Garze terrane. (d) Post-Oligocene–early Pliocene time. Erosional planation of early Tertiary fault-bounded basin occurs in western Songpan Garze terrane. Reactivation of Longmen Shan and Yalong thrust belts occur with speculative minor flexural subsidence and foreland basin deposition. Folding of early Tertiary sediments occurs in the Chuxiong and Daliang basins that accommodate 20–25 km shortening, similar to the post-Oligocene horizontal offsets of the Longmen Shan thrust belt. Magnitude of surface shortening is insufficient to explain total crustal thickening. Also, surface shortening is limited to a narrow region of the plateau margin and cannot explain crustal thickening that has occurred across distances of >1000 km into the eastern foreland. Erosional planation of much of the Yalong thrust belt and folded basin sediments occurs prior to Pliocene time. High elevations develop in the Longmen Shan and in the southeastern plateau margin by late middle-Miocene time. Major crustal thickening and lateral plateau growth is coeval with or postdates Tertiary record of horizontal shortening. Strike-slip faulting dominates the late Tertiary active tectonics.

protect large areas from fluvial dissection. Orographic effects following plateau growth may also serve to keep precipitation focused at lower elevations (<3 km), effectively starving the headwater regions of precipitation and aiding slow retreat of knickpoints toward the central plateau.

[55] The most significant disruption of the relict landscape occurs across the Longmen Shan. The surface of the Sichuan Basin has been an erosional landscape throughout Cenozoic time, during which deposition has been limited to thin deposits in the southwestern portion of the basin that are being presently incised. Detrital apatite fission track ages (AFT) from Mesozoic sedimentary deposits are near their depositional age, and the lack of Cenozoic age resetting of the AFT ages suggests that less than a few

kilometers of burial and exhumation of these rocks occurred since Cretaceous time [*Arne et al.*, 1997]. Although this inference remains controversial based on borehole AFT data interpreted by *Xu and Kamp* [2000], minimal sedimentation in the Sichuan Basin is consistent with cooling rates determined from thermochronologic dating indicate that slow exhumation rates and subdued topography existed across the Longmen Shan escarpment from Jurassic time to at least 12 Ma, because slow cooling implies slow denudation rates and because slow denudation in the presence of extreme topographic gradients requires extremely nonerosive climate conditions that are unreasonable for central Asia in Miocene time. Thus rapid cooling that began between 12 and 5 Ma in the Longmen Shan reflects increased exhumation rates associated with the development of steep topographic gradients [*Kirby et al.*, 2002].

8. Implications for Crustal Dynamics

[56] Relict landscape formation and eventual destruction by fluvial dissection provides timing and magnitude estimates of plateau growth. While the relict landscape formed at different times in different areas, Paleocene to Oligocene age rocks deposited and subsequently deformed were eventually beveled by erosion as the low-relief landscape was reestablished prior to Late Miocene–Pliocene time, constrained by the age of flat-lying sediments that mantle the surface in patches. Local vertical offsets of remnant surfaces across late Miocene and younger strike-slip and normal faults [*Wang et al.*, 1998] suggest that the surface is older than these structures (>8 Ma). These data are consistent with isotopic ages from river gorges that indicate a late Miocene (9–13 Ma) age for the abandonment of the relict landscape by initiation of rapid river incision, and with isotopic ages from the Longmen Shan that suggest development of a steep topographic escarpment by late Miocene time [*Kirby et al.*, 2002]. Taken together, these data suggest that southeastern plateau remained at low-elevation until Miocene, probably late Miocene time.

[57] While Himalayan-scale fold and thrust belt deformation is absent along the southeastern plateau in Cenozoic time, we cannot exclude the possibility that horizontal deformation accommodated in the Longmen Shan/Yalong thrust belt and in isolated areas throughout the southeastern plateau contributed to crustal thickening and an increase in plateau elevation. Facies relationships of offset Oligocene sedimentary rocks constrain shortening in the Longmen Shan to a few tens of kilometers, however Cenozoic age shortening in the Yalong Thrust Belt is unknown. The Yalong thrust belt coincides with an area where the relict landscape surface has a steeper dip than is observed elsewhere along the gently dipping plateau margin (Figure 11c). In this region, there is relatively poor preservation of relict landscape patches compared to regions to the north and south. South of this steep zone in the relict landscape, there is a swath of thin, coarse clastic deposits (mostly a few hundred meters thick, but locally up to 1–2 km) that are early – mid? Tertiary age, locally dated as Late Eocene [*BGMRS*, 1991; *BGMRY*, 1990; *Si et al.*, 2000]. We speculate that the juxtaposition of an area of steeper slopes in the paleosurface, and greater dissection of the relict landscape may represent a shallow, foredeep basin adjacent to an older, incipient plateau margin. However, the regional elevation must have been much less than today, because these deformed sediments were erosionally beveled to low-relief and capped unconformably by Pliocene age rocks. Furthermore, erosional planation of the early Tertiary deformation throughout the southeastern Tibetan Plateau suggests that this deformation predates major crustal thickening.

[58] The mechanism and timing by which the high topography and thick crust of Tibet expanded laterally bears on our understanding of crustal dynamics during continental deformation. The relict landscape of the eastern plateau provides a measure of vertical displacement, which we interpret as a direct consequence of crustal thickening because topographic contours parallel gradients in crustal thickness [*Li and Mooney*, 1998]. The transition between steep and gently dipping plateau margins does not appear to be related to preexisting (Mesozoic–early Tertiary) structure nor to crustal terrane boundaries because the Sichuan Basin and adjacent areas beneath the gently dipping plateau margins are both underlain by Proterozoic basement rocks of the Yangtze Craton. However, the Sichuan Basin occupies a part of the Yangtze craton that has escaped earlier Mesozoic deformation while rocks surrounding the basin were deformed at various times. The magnitude of vertical displacement correlates with seismic anomalies in the lower crust and mantle and with surface heat flow: displacements are large where heat flow is high and seismic wave speeds are slow, and nonexistent where heat flow is low and seismic wave speeds are fast [*Lebedev and Nolet*, 2003; *Hu et al.*, 2000]. As well, the long-wavelength tilt of the reconstructed relict landscape mirrors the low-gradient decrease in crustal thickness across the plateau margin [*Li and Mooney*, 1998] (Figure 3). This suggests that crustal thickening and an increase in surface elevation occur only where the lower crust and/or upper mantle is hot and/or fluid rich. Smoothly varying surface topography above a region of hot, thickened crust where the horizontal shortening of the crust is minor, is consistent with the concept that crustal thickening beneath the eastern plateau occurred by eastward ductile flow of deep crustal material. In our interpretation, the location of the steep plateau margin is controlled by the deep rheology of the lithosphere beneath the Sichuan Basin, so that eastward flow of crustal material is interrupted and forced to flow around the basin, forming the region of distributed crustal thickening and smoothly distributed regional elevation gradients.

9. Conclusion

[59] Low-relief erosional surfaces have been described in nearly every active orogen [e.g., *Lawson*, 1936; *Webb*, 1946; *Epis and Chapin*, 1975; *Gansser*, 1983; *Gubbels et al.*, 1993; *Chapin and Kelley*, 1997; *Abbott et al.*, 1997; *Sugai and Ohmori*, 1999]. Where present, they are records of changing boundary conditions (tectonic or climatic) preserved in the modern topography. Erosion surfaces, especially large-scale relict landscapes as described in this paper, can be used to measure vertical deformation, as W. M. Davis envisioned more than 100 years ago [*Davis*, 1899], however, certain conditions need apply. Surfaces need to be of fluvial origin and a part of the modern fluvial

system, because river systems grade to a common base level elevation. This condition allows one to argue that adjacent surface remnants were formed at similar elevations. Modification of surfaces by erosion must be demonstrably slow enough to allow surfaces to be used as a passive marker proxy of elevation change. Low-relief landscapes can form at any elevation and need not have graded to sea level nor be a marker of absolute elevation change, however demonstration that local base level was paleosea level satisfies this condition. Finally, large-scale, low-relief, relict landscapes need not have formed at the same time in order to be used as a paleosurface. Only the observation that a regional landscape of low-relief existed at some time in the past is essential, even if some parts were formed earlier than others or were reworked.

[60] The application of these criteria in geomorphic studies offers the potential to measure vertical deformation of the Earth's surface over 10^6–10^7 year timescales, providing paleo-elevation data for tectonic and geodynamic studies that is difficult to obtain by other methods. These applications depend critically on the ability to distinguish between a part of the landscape that has or is in the process of responding to new conditions (''active landscape'') and a part of the landscape that has not (''relict landscape''). In this paper, we outline criteria that can be used to make this distinction from geologic and geomorphic constraints derived from digital data and field observations. We focus on the circumstance where a relict landscape is recognized by subdued relief and erosion processes associated with slow erosion rates in the headwater regions of major rivers and tributaries, that contrast with an active landscape characterized by high relief and rapid erosion rates concentrated in trunk streams and the lower portions of major tributaries. We argue that this type of morphologic contrast represents a transient landscape response to an increase in elevation and/or rock uplift rate and that the change in elevation of the relict landscape provides a measure of long-term vertical deformation.

[61] Continuity of a relict landscape along the eastern Tibetan Plateau margin from high to low elevation and a lack of correlation to a particular lithology or tectonic province is used to test the hypothesis that remnant surfaces collectively comprise an elevated paleolandscape. The change in elevation of this paleolandscape produces a vertical deformation map of 3–4 km of uplift (elevation gain) beneath the high-elevation eastern plateau that gently decreases to the southeast toward the South China Sea. Because the appropriate age and magnitude shortening structures that one would typically exploit for the timing and geometry of lateral plateau growth are generally lacking along the eastern Tibetan Plateau margin, the recognition of an elevated, relict landscape has been critical to our understanding of the tectonic evolution. The diachroneity of erosional and depositional processes that were involved in forming the relict landscape largely occurred prior to deep incision of the modern river system into the elevated relict landscape, therefore incision of deep river gorges into an elevated relict landscape has provided context for using river incision as a proxy for initiation of plateau rise at 9–13 Ma [*Clark et al.*, 2005b]. Smoothly varying, southeastward plateau growth is determined from the change in elevation of the relict landscape remnants, suggesting distributed, rather than stepwise, eastward growth of the plateau. The fact that the reconstructed paleolandscape dips gently to the southeast, mirroring the southeastward decrease in crustal thickness, is significant because it suggests that plateau growth of the eastern margin is related to southeastward directed crustal thickening. This orientation of crustal thickening and surface rise is perpendicular to expected shortening directions predicted by the north-northeastward plate convergence between India and Eurasia. Southeastward flow of weak, deep crustal material driven by lateral pressure gradients in crustal thickness between the central plateau and the foreland regions may explain smooth, regional-scale elevation change and the unusual southeastward orientation of plateau growth (Figure 3b).

[62] Constraints on the age of the paleolandscape and its destruction by river incision indicate that mass transfer via lower crustal flow is largely late Miocene age and younger. These data indicate that the magnitude of material flux through the lower crust of southeastern Tibet is probably unusually fast, perhaps coincident with a zone of unusually weak mid or lower crustal rocks that may be due in part to elevated crustal geotherms, crustal fluids, and/or thick sedimentary sequences [*Royden et al.*, 1997; *Clark and Royden*, 2000; *Shen et al.*, 2001; *Clark et al.*, 2005a]. The pattern of surface uplift interpreted from the relict landscape suggests that the mobilization of deep crustal material has occurred independent of the pattern of strain recorded in the upper crust since 9–13 Ma. The lack of correlation between the orientation, style and magnitude of structure in the upper crust and the pattern of crustal thickening determined from the relict landscape suggests that the upper and lower crust in southeastern Tibet are poorly coupled since mid-Miocene time. Young strike-slip faults present in southeastern Tibet, with up to 60 km of late Miocene to Quaternary displacement, do not produce significant disruption of the relict landscape in a vertical sense. These strike-slip faults, which dominate the surface strain of eastern Tibet over the past 8–10 Ma, are probably also poorly coupled to the lower crust and probably sole into or end within a zone of weak lower crust. Thus a model of viscous deformation concentrated in the deep crust explains much of the pattern of young eastward growth of the Tibetan Plateau, which has occurred independently of the structural history of the upper crust since at least late Miocene time.

[63] **Acknowledgments.** This work was supported by the NSF Continental Dynamics program (EAR-9614970, EAR-9814303) (L.H., B.C.B., and K.X.W.) and a NSF graduate fellowship (M.K.C.). We thank Zhiliang Chen, drivers and staff at the Chengdu Institute of Geology and Mineral Resources, Katra Andreini, and Martha House for their expertise and support during our field campaigns. We also thank S. Brocklehurst, B. Crosby, E. Kirby, W. Ouimet, L. Schoenbohm, and N. Snyder for thoughtful discussions on the subject of regional-scale erosion surfaces. The detailed and constructive reviews by A. Densmore (Associate Editor), P. Molnar, and J. Spotila greatly improved the clarity of this manuscript.

References

Abbott, L. D., E. A. Silver, R. S. Anderson, R. Smith, J. C. Ingle, S. A. Kling, D. Haig, E. Small, J. Galewsky, and W. Sliter (1997), Measurement of tectonic surface uplift rate in a young collisional mountain belt, *Nature*, *385*, 501–507.

Akciz, S. (2004), Structural and geochronological constraints on the ductile deformation observed along the Gaoligong Shan and Chong Shan shear zones, Yunnan (China), Ph.D. thesis, 211 pp., Mass. Inst. of Technol., Cambridge.

Akciz, S., B. C. Burchfiel, L. Chen, and J. Yin (2001), Geometry, kinematics and regional significance of the Chong Shan shear zone, Yunnan, China, *Geol. Soc. Am. Abstr. Programs*, *33*(6), 395.

Arne, D., B. Worley, C. Wilson, S. Chen, D. Foster, Z. Luo, S. Liu, and P. Dirks (1997), Differential exhumation in response to episodic thrusting along the eastern margin of the Tibetan Plateau, *Tectonophysics*, *280*, 239–256.

Barbour, G. B. (1936), Physiographic history of the Yangtze, *Geogr. J.*, *87*, 17–34.

Burchfiel, B. C., Z. Chen, Y. Liu, and L. H. Royden (1995), Tectonics of the Longmen Shan and adjacent regions, central China, *Int. Geol. Rev.*, *37*, 661–735.

Bureau of Geology and Mineral Resources of Sichuan Province (BGMRS) (1991), *Regional Geology of Sichuan Province*, 730 pp., Geol. Publ. House, Beijing.

Bureau of Geological and Mineral Resources of Yunnan Province (BGMRY) (1990), *Regional Geology of Yunnan Province*, 728 pp., Geol. Publ. House, Beijing.

Chapin, C. E., and S. A. Kelley (1997), The Rocky Mountain erosion surface in the front range of Colorado, in *Colorado Front Range Guidebook 1997*, pp. 101–113, Rocky Mtn. Assoc. of Geol., Denver, Colo.

Chen, S. F., and C. J. L. Wilson (1996), Emplacement of the Longmen Shan Thrust-Nappe Belt along the eastern margin of the Tibetan Plateau, *J. Struct. Geol.*, *18*, 413–430.

Chen, S. F., C. J. L. Wilson, and B. A. Worley (1995), Tectonic transition from the Songpan-Garze Fold Belt to the Sichuan Basin, south-western China, *Basin Res.*, *7*, 235–253.

Chen, Z., B. C. Burchfiel, Y. Liu, R. W. King, L. H. Royden, W. Tang, E. Wang, J. Zhao, and X. Zhang (2000), GPS measurements from eastern Tibet and their implications for India/Eurasia intercontinental deformation, *J. Geophys. Res.*, *105*, 16,215–16,227.

Clark, M. K., and L. H. Royden (2000), Topographic ooze: Building the eastern margin of Tibet by lower crustal flow, *Geology*, *28*, 703–706.

Clark, M. K., L. Schoenbohm, L. H. Royden, K. X. Whipple, B. C. Burchfiel, X. Zhang, W. Tang, E. Wang, and L. Chen (2004), Surface uplift, tectonics, and erosion of eastern Tibet as inferred from large-scale drainage patterns, *Tectonics*, *23*, TC1006, doi:10.1029/2002TC001402.

Clark, M. K., J. W. M. Bush, and L. H. Royden (2005a), Dynamic topography produced by lower crustal flow against rheologic strength heterogeneities bordering the Tibetan Plateau, *Geophys. J. Int.*, 575–590, doi:10.1111/j.1365-246x.2005.02580.x.

Clark, M. K., M. A. House, L. H. Royden, K. X. Whipple, B. C. Burchfiel, X. Zhang, and W. Tang (2005b), Late Cenozoic uplift of eastern Tibet, *Geology*, *33*, 525–528, doi:10.1130/G21265.1.

Davis, W. M. (1899), The geographic cycle, *Geogr. J.*, *14*, 481–504.

Dirks, P. H. G. M., C. J. L. Wilson, S. Chen, Z. L. Luo, and S. Liu (1994), Tectonic evolution of the NE margin of the Tibetan Plateau: Evidence from the central Longmen Mountains, Sichuan Province, China, *J. Southeast Asian Earth Sci.*, *9*(1–2), 181–192.

Epis, R. C., and C. E. Chapin (1975), Geomorphic and tectonic implications of the post-Laramide, late Eocene erosion surface in the southern Rocky Mountains, *Mem. Geol. Soc. Am.*, *144*, 45–74.

Fielding, E. (1996), Tibet uplift and erosion, *Tectonophysics*, *260*, 55–84.

Gansser, A. (1983), *Geology of the Bhutan Himalaya*, *Denkschr. Schweiz. Naturforsch. Ges. Basel*, vol. 96, 181 pp., Springer, New York.

Gilley, L. D., T. M. Harrison, P. H. Leloup, F. J. Ryerson, O. M. Lovera, and J.-H. Wang (2003), Direct dating of left-lateral deformation along the Red River shear zone, China and Vietnam, *J. Geophys. Res.*, *108*(B2), 2127, doi:10.1029/2001JB001726.

Gregory, J. W., and C. J. Gregory (1925), The geology and physical geography of Chinese Tibet, and its relations to the mountain system of south-eastern Asia, from observations made during the Percy Sladen Expedition (1922), *Philos. Trans. R. Soc. London, Ser. B*, *213*, 171–298.

Gubbels, T. L., B. L. Isacks, and E. Farrar (1993), High-level surfaces, plateau uplift, and foreland development, Bolivian central Andes, *Geology*, *21*, 695–698.

Hallet, B., and P. Molnar (2001), Distorted drainage basins as markers of crustal strain east of the Himalaya, *J. Geophys. Res.*, *106*, 13,697–13,709.

Harrowfield, M. J., and C. J. L. Wilson (2005), Indosinian deformation of the Songpan Garze Fold Belt, northeast Tibetan Plateau, *J. Struct., Geol.*, *27*, 101–107.

Horton, B. K., A. Yin, M. S. Spurlin, and J. Wang (2002), Paleocene–Eocene syncontractional sedimentation in narrow, lacustrine-dominated basins of east-central Tibet, *Geol. Soc. Am. Bull.*, *114*, 771–786.

Hu, S., L. He, and J. Wang (2000), Heat flow in the continental area of China: A new data set, *Earth Planet. Sci. Lett.*, *179*, 407–419.

Huang, M.-H., I. S. Buick, and L. W. Hou (2003), Tectonometamorphic evolution of the eastern Tibet Plateau: Evidence from the central Songpan-Garze orogenic belt, western China, *J. Pet.*, *44*, 255–278.

Jordan, T. A., and A. B. Watts (2005), Gravity anomalies, flexure and the elastic thickness structure of the India-Eurasia collisional system, *Earth Planet. Sci. Lett.*, *236*(3–4), 732–750.

King, R. W., F. Shen, B. C. Burchfiel, L. H. Royden, E. Wang, Z. Chen, Y. Liu, X. Zhang, J. Xhao, and Y. Li (1997), Geodetic measurement of crustal motion in southwest China, *Geology*, *25*, 79–182.

Kirby, E., and K. X. Whipple (2001), Quantifying differential rock-uplift rates via stream profile analysis, *Geology*, *29*, 415–418.

Kirby, E., P. W. Reiners, M. A. Krol, K. X. Whipple, K. V. Hodges, K. A. Farley, W. Tang, and Z. Chen (2002), Late Cenozoic evolution of the eastern margin of the Tibetan Plateau: Inferences from $^{40}Ar/^{39}Ar$ and (U-Th)/He thermochronology, *Tectonics*, *21*(1), 1001, doi:10.1029/2000TC001246.

Kirby, E., K. X. Whipple, W. Tang, and Z. Chen (2003), Distribution of active rock uplift along the eastern margin of the Tibetan Plateau: Inferences from bedrock channel longitudinal profiles, *J. Geophys. Res.*, *108*(B4), 2217, doi:10.1029/2001JB000861.

Lacassin, R., U. Scharer, P. H. Leloup, N. Arnaud, P. Tapponnier, X. Liu, and L. Zhang (1996), Tertiary deformation and metamorphism SE of Tibet: The folded Tiger-leap decollement of NW Yunnan, China, *Tectonics*, *15*, 605–622.

Lawson, A. C. (1936), The Sierra Nevada in the light of isostasy, *Geol. Soc. Am. Bull.*, *47*, 1691–1712.

Lebedev, S., and G. Nolet (2003), The upper mantle beneath SE Asia from S-velocity tomography, *J. Geophys. Res.*, *108*(B1), 2048, doi:10.1029/2000JB000073.

Lehmkuhl, F. (1998), Extent and spatial distribution of Pleistocene glaciations in eastern Tibet, *Quat. Int.*, *45-6*, 123–134.

Leloup, P. H., T. M. Harrison, F. J. Ryerson, W. Chen, Q. Li, P. Tapponnier, and R. Lacassin (1995), The Ailao Shan-Red River shear zone (Yunnan, China), Tertiary transform boundary of Indochina, *Tectonophsyics*, *251*, 3–84.

Leloup, P. H., N. Arnaud, R. Lacassin, J. R. Kienast, T. M. Harrison, T. T. Phan Trong, A. Replumaz, and P. Tapponnier (2001), New constraints on the structure, thermochronology, and timing of the Ailao Shan-Red River shear zone, SE Asia, *J. Geophys. Res.*, *106*, 6683–6732.

Li, S., and W. D. Mooney (1998), Crustal structure of China from deep sounding profiles, *Tectonophysics*, *288*, 105–113.

Li, Y., P. A. Allen, A. L. Densmore, and X. Qiang (2003), Evolution of the Longmen Shan Foreland Basin (western Sichuan, China) during the Late Triassic Indosinian orogeny, *Basin Res.*, *15*, 117–138.

Masek, J. G., B. L. Isacks, E. J. Fielding, and J. Browaeys (1994), Rift flank uplift in Tibet: Evidence for a viscous lower crust, *Tectonics*, *13*, 659–667.

Mattauer, M., J. Malavieille, S. Calassou, J. Lancelot, F. Roger, Z. Hao, Z. Xu, and L. Hou (1992), La chaîne Triasique de Songpan-Garze (ouest Sichuan et est Tibet): Une chaîne de plissement-décollement sur marge passive, *C. R. Acad. Sci. Paris, Ser. II*, *314*, 619–626.

Meng, Q.-R., E. Wang, and J.-M. Hu (2005), Mesozoic sedimentary evolution of the northwest Sichuan basin: Implication for continued clockwise rotation of the South China block, *Geol. Soc. Am. Bull.*, *117*, 396–410, doi:10.1130/B25407.1.

Merritts, D., and M. Ellis (1994), Introduction to special section on tectonics and topography, *J. Geophys. Res.*, *99*, 12,135–12,141.

Niemi, N. A., M. K. Clark, M. A. House, L. H. Royden, and X. Zhang (2003), Late Cenozoic extension and exhumation of mid-crustal rocks at Gonga Shan, eastern Tibet, *Geophys. Res. Abstr.*, *5*, Abstract 12918.

Ouimet, W., and K. Whipple (2004), Mega-landslides in eastern Tibet: Implications for landscape and river profile evolution, and the interpretation of tectonics from topography, *Eos Trans. AGU*, *85*(47), Fall Meet. Suppl., Abstract H44A-04.

Ouimet, W., K. X. Whipple, L. H. Royden, and D. Granger (2005), Long transient response times of rivers in eastern Tibet to regional plateau uplift: The effect of mega-landslides, *Geophys. Res. Abstr.*, *7*, Abstract 05743.

Reid, A. J., C. J. L. Wilson, and S. Liu (2005a), Structural evidence for the Permo-Triassic tectonic evolution of the Yidun Arc, eastern Tibetan Plateau, *J. Struct. Geol.*, *27*, 119–137.

Reid, A. J., C. J. L. Wilson, D. Phillips, and S. Liu (2005b), Mesozoic cooling across the Yidun Arc, central-eastern Tibetan Plateau: A reconnaissance $^{40}Ar/^{39}Ar$ study, *Tectonophysics*, *398*, 45–66.

Roger, F. (1994), Datation et tracage des granitoïdes associes a la chaine de Songpan Garze (W Sichuan, Chine) par les methodes: U-Pb, Rb-Sr et Sm-Nd, Ph.D. thesis, Univ. Montpellier II, Montpellier, France.

Roger, F., S. Calassou, J. Lancelot, J. Malavieille, M. Mattauer, Z. Xu, Z. Hao, and L. Hou (1995), Miocene emplacement and deformation of the Konga Shan granite (Xianshui He fault zone, west Sichuan, China): Geodynamic implications, *Earth Planet. Sci. Lett.*, *130*, 201–216.

Royden, L. H., B. C. Burchfiel, R. W. King, E. Wang, Z. Chen, F. Shen, and L. Yuping (1997), Surface deformation and lower crustal flow in eastern Tibet, *Science*, *276*, 788–790.

Schoenbohm, L., K. X. Whipple, B. C. Burchfiel, and L. Chen (2004), Geomorphic constraints on surface uplift, exhumation, and plateau growth in the Red River region, Yunnan Province, China, *Geol. Soc. Am. Bull.*, *116*, 895–909, doi:10.1130/B25364.

Shen, F., L. H. Royden, and B. C. Burchfiel (2001), Large-scale crustal deformation of the Tibetan Plateau, *J. Geophys. Res.*, *106*, 6793–6816.

Si, G., Y. Li, and Z. Hou (2000), The Tertiary stratigraphy sequence of Yanyuan Basin in the southeastern margin of the Qinghai-Tibet Plateau, *Earth Sci. Frontiers*, *7*, 304–305.

Spotila, J. A., and K. Sieh (2000), Architecture of transpressional thrust faulting in the San Bernardino Mountains, southern California, from deformation of a deeply weathered surface, *Tectonics*, *19*, 589–615.

Sugai, T., and H. Ohmori (1999), A model of relief forming by tectonic uplift and valley incision in orogenesis, *Basin Res.*, *11*, 43–57.

Tapponnier, P., X. Zhiqin, F. Roger, B. Meyer, N. Arnaud, G. Wittlinger, and Y. Jingsui (2001), Oblique stepwise rise and growth of the Tibet Plateau, *Science*, *294*, 1671–1677.

Tregar, T. R. (1965), *A Geography of China*, 342 pp., Univ. of London Press, London.

U.S. Geological Survey (1993), Digital elevation models: Data users guide 5, report, 50 pp., Reston, Va.

Von Lóczy, L. (1893), *Die beschreibung der geologischen beobachtungen und deren resultate der reise des grafen Béla Széchenyi in ostasien*, 847 pp., Ed. Hölzel, Vienna.

Wallis, S., T. Tsujimor, M. Aoya, T. Kawakami, K. Terada, K. Suzuki, and H. Hyodo (2003), Cenozoic and Mesozoic metamorphism in the Longmenshan orogen: Implications for geodynamic models of eastern Tibet, *Geology*, *31*, 745–748.

Wang, E., and B. C. Burchfiel (1997), Interpretation of Cenozoic tectonics in the right-lateral accommodation zone between the Ailao Shan Shear Zone and the eastern Himalayan syntaxis, *Int. Geol. Rev.*, *39*, 191–219.

Wang, E., B. C. Burchfiel, L. H. Royden, L. Chen, J. Chen, W. Li, and Z. Chen (1998), Late Cenozoic Xianshuihe-Xiaojiang, Red River, and Dali fault systems of southwestern Sichuan and central Yunnan, China, *Spec. Pap. Geol. Soc. Am.*, *327*, 108 pp.

Webb, R. W. (1946), The geomorphology of the Middle Kern River Basin, southern Sierra Nevada, California, *Geol. Soc. Am. Bull.*, *57*, 355–382.

Whipple, K. X., and G. E. Tucker (1999), Dynamics of the stream-power river incision model: Implications for height limits of mountain ranges, landscape response timescales and research needs, *J. Geophys. Res.*, *104*, 17,661–17,674.

Whipple, K. X., E. Kirby, and S. H. Brocklehurst (1999), Geomorphic limits to climatically induced increases in topographic relief, *Nature*, *401*, 39–43.

Widdowson, M. (1997), The geomorphological and geological importance of palaeosurfaces, in *Palaeosurfaces: Recognition, Reconstruction and Palaeoenvironmental Interpretation*, *Spec. Publ. Geol. Soc.*, *120*, 1–12.

Wobus, C., K. X. Whipple, E. Kirby, N. Snyder, J. Johnson, K. Spyropolou, B. Crosby, and D. Sheehan (2006), Tectonics from topography: Procedures, promise and pitfalls, in *Tectonics, Climate and Landscape Evolution*, edited by S. D. Willet et al., *Spec. Pap. Geol. Soc. Am.*, *398*, 55–74, doi:10.1130/2006.2398(04).

Xu, G. (1997), Thermo-tectonic history of eastern Tibetan Plateau and western Sichuan Basin, China, assessed by fission track thermochronology, Ph.D. thesis, 353 pp., Univ. of Waikato, Hamilton, New Zealand.

Xu, G., and P. Kamp (2000), Tectonics and denudation adjacent to the Xianshuihe Fault, eastern Tibetan Plateau: Constraints from fission-track thermochronology, *J. Geophys. Res.*, *105*, 19,231–19,251.

B. C. Burchfiel, L. H. Royden, and K. X. Whipple, Department of Earth, Atmospheric and Planetary Sciences, Massachusetts Institute of Technology, Cambridge, MA 02139, USA.

M. K. Clark, Department of Geological Sciences, University of Michigan, 1100 North University Avenue, Ann Arbor, MI 48109, USA. (marinkc@umich.edu)

W. Tang and X. Zhang, Chengdu Institute of Geology and Mineral Resources, Chengdu, 610082, China.